Control of lens development by Lhx2-regulated neuroretinal FGFs.

Thuzar Thein[1], Jimmy de Melo[1], Cristina Zibetti[1], Brian S Clark[1], Felicia Juarez[1], and Seth Blackshaw[1-5]

[1]Solomon H. Snyder Department of Neuroscience, [2]Department of Ophthalmology, [3]Department of Neurology, [4]Center for Human Systems Biology, and [5]Institute for Cell Engineering, Johns Hopkins University School of Medicine, 733 N. Broadway, Baltimore, MD, USA

Summary Statement

The LIM homeodomain transcription factor Lhx2 regulates neuroretinal-derived FGFs – FGF3, FGF9 and FGF15 – essential for lens cell proliferation, survival and differentiation.

Abstract

Fibroblast growth factor (FGF) signaling is an essential regulator of lens epithelial cell proliferation and survival, as well as lens fiber cell differentiation. However, the identities of these FGF factors, their source tissue, and the genes that regulate their synthesis are unknown. We have found that *Chx10-Cre;Lhx2*$^{lox/lox}$ mice, which selectively lack Lhx2 expression in neuroretina from E10.5, showed an early arrest in lens fiber development along with severe microphthalmia. These mutant animals showed reduced expression of multiple neuroretina-expressed FGFs and canonical FGF-regulated genes in neuroretina. When FGF expression was genetically restored in *Lhx2*-deficient neuroretina of *Chx10-Cre;Lhx2*$^{lox/lox}$ mice, we observed a partial but nonetheless substantial rescue of the defects in lens cell proliferation, survival and fiber differentiation. These data demonstrate that neuroretinal expression of Lhx2 and neuroretina-derived FGF factors are crucial for lens fiber development *in vivo*.

Introduction

Vertebrate lens development has long been a model system for studying the role of inductive signaling in tissue patterning and cell specification (Gunhaga, 2011). During embryogenesis, the surface ectoderm adjacent to the optic vesicle thickens and invaginates to give rise to the lens vesicle. Subsequently, cells in the anterior lens vesicle become a monolayer of lens epithelial cells, while cells in the posterior half of the vesicle elongate and differentiate to form primary lens fibers, which fill the lens vesicle. After this distinctive architecture has been established, lens growth continues in a spatially restricted manner maintaining lens polarity. Lens epithelial cells proliferate in the germinative zone, the region just above the lens equator. The progeny then migrate or are displaced below the equator into the transitional zone where they exit the cell cycle, elongate and differentiate into secondary fiber cells (Lovicu and Robinson, 2004; McAvoy et al., 1999).

Previous work has shown that the differentiation of lens epithelial cells into fiber cells is dependent on diffusible signals from the neuroretina (Coulombre and Coulombre, 1963; McAvoy and Fernon, 1984; Yamamoto, 1976). However, the identity of these retinal-derived factors remains unclear. Multiple growth factors have been implicated in control of lens fiber differentiation (Lovicu et al., 2011; Lovicu and McAvoy, 2005; Wang et al., 2010). FGFs have long been a top candidate among these, following landmark studies demonstrating that treatment of cultured lens epithelial cells with FGF1 and 2 was sufficient to induce differentiation into lens fiber cells (Chamberlain and McAvoy, 1987, 1989). Subsequent studies have provided compelling evidence that FGFs promote lens epithelial cell proliferation and fiber cell differentiation in a dose-dependent manner (Lovicu and McAvoy, 2005; McAvoy and Chamberlain, 1989; Schulz et al., 1993). While this stimulated speculation that FGFs might be the long-sought neuroretina-derived signal, targeted mutation studies carried out over the last several decades have yet to identify any specific FGFs that are necessary, either individually or in combination, for lens cell proliferation or differentiation (Robinson, 2006). More recently, targeted deletion of three FGF receptors (*Fgfr1-3*) in lens pit/vesicle have been shown to disrupt lens cell survival and fiber cell differentiation. However, individual or pairwise deletion of FGF receptor genes still resulted in grossly normal lens formation (Zhao et al., 2008). This functional redundancy of FGF receptors suggests that multiple FGFs act in concert to promote lens fiber differentiation. The identities and source of these factors, however, remain obscure.

Lhx2 is a LIM-homeodomain transcription factor essential for eye development. A previous study has shown that lens development arrests at, or just prior to, lens placode formation in *Lhx2* germline mutant animals. FGF15, BMP4, BMP7 and phosphorylated SMAD1, 5 and 8 (pSMAD1/5/8), a read-out of BMP signaling, are all downregulated in the *Lhx2*$^{-/-}$ optic neuroepithelium and lens-forming region of the surface ectoderm. Restoration of BMP4 and BMP7 led to upregulation of FGF15 in the optic neuroepithelium and induction of the lens placode marker Sox2 in the surface ectoderm of *Lhx2*$^{-/-}$ animals. But BMP treatment does not rescue the morphology of *Lhx2*$^{-/-}$ mutant optic vesicle or surface ectoderm. These findings suggest that BMP signaling partially mediates Lhx2-dependent regulation of optic vesicle and lens vesicle induction (Yun et al., 2009). However, if Lhx2 is required for lens development past lens placode formation is not known.

We recently observed that selective deletion of the Lhx2 in neuroretina after lens placode induction led to severe microphthalmia and a near-total loss of the expression of many retinal progenitor-specific genes (Roy et al., 2013). Interestingly, we also noticed severe disruptions of lens development in these animals. This suggested that Lhx2 may regulate the expression of neuroretina-derived diffusible factors that are necessary for lens development past lens placode stage. To address this possibility, we set out to identify

candidate factors whose expression was disrupted in Lhx2-deficient neuroretina, and to determine whether restoring the activity of these factors was sufficient to rescue lens cell proliferation and fiber differentiation.

Results

Selective deletion of Lhx2 in embryonic neuroretina disrupts lens development

We observed that selective deletion of Lhx2 in neuroretina using *Chx10-Cre* resulted in severe microphthalmia in adult mice (Fig. 1 *A* and *B*). Close examination of *Chx10-Cre;Lhx2*$^{lox/lox}$ eye sections revealed severe defects in lens development at embryonic day (E)13.5 as well as postnatal day (P)0.5 (Fig. 1 *C* – *F*). The lens was either missing altogether, or detectable only as a vestigial lumen rudiment (Fig. 1 *D* and *F*). Lens size was reduced to a substantially greater extent (740-fold smaller) than retinal size (7.3-fold smaller) at P0.5 (Fig. 1 *G*). Analysis of *Chx10-Cre;Ai9*(*Rosa26*$^{LSL\text{-}tdTomato}$) mice confirmed previous reports (Rowan and Cepko, 2004) that this Cre line is selectively active in neuroretina, and not active in other ocular tissues, including lens (Fig. S1 *A* – *D*). Immunostaining for Lhx2 showed selective deletion of Lhx2 in neuroretina starting at E10.5 with the expression almost entirely lost in neuroretina by E11.5 (Fig. S1 *E* – *L*). Even though some Lhx2 staining was observed in both control and mutant lenses, signals were never detected in the nuclei of lens cells. Moreover, *Lhx2* mRNA was also never detected in either control or *Chx10-Cre;Lhx2*$^{lox/lox}$ lenses (insets in Fig. 2). Since previous work has shown that Lhx2 expression is absent in the lens at all stages of ocular development (Hägglund et al., 2011), we conclude that the Lhx2 signal observed in the lens here represents non-specific background staining. Furthermore, as the Cre is active only in the neuroretina of our animals, we conclude that the disruption of lens development observed in our *Chx10-Cre;Lhx2*$^{lox/lox}$ animals must have resulted from disrupted signaling by secreted retinal-derived factors.

FGF signaling is downregulated in Lhx2-deficient eyes

To identify candidate retinal-derived factors whose expression was altered in *Lhx2*-deficient neuroretina, we analyzed previously reported microarray data obtained from retinas of control and *Chx10-Cre;Lhx2*$^{lox/lox}$ mice at E13.5 (Roy et al., 2013). These data indicated that multiple different FGFs and FGF-regulated genes showed altered expression in *Chx10-Cre;Lhx2*$^{lox/lox}$ retina (Fig. 2*A*). *Fgf3*, *Fgf9*, and *Fgf15* – all of which have previously been reported to be expressed in embryonic neuroretinal progenitors (Colvin et al., 1999; Kurose et al., 2004; Wilkinson et al., 1989) – were dramatically downregulated. FGF-regulated genes, *Etv5* and *Spry2*, were also downregulated, while FGF receptor gene, *Fgfr3*, was upregulated. Loss of *Fgf3*, *Fgf9* and *Fgf15* expression in *Chx10-Cre;Lhx2*$^{lox/lox}$ retinas at E13.5 was confirmed using qRT-PCR and *in situ* hybridization analysis (Fig. 2 *B* – H). *In situ* hybridization analysis at E13.5 showed a reduction in the expression of the FGF-regulated genes *Etv5*, *Etv1* and *Spry2* in the lenses of *Chx10-Cre;Lhx2*$^{lox/lox}$ mice (Fig. 3 *I, K, M, O, Q* and *S*). Taken together, these data suggested that loss of expression of multiple different FGF genes in *Chx10-Cre;Lhx2*$^{lox/lox}$ retinas resulted in a global loss of FGF signaling in the lenses.

Forced expression of FGF10 in neuroretina induces FGF-regulated genes in the lens

Since FGFs typically signal through multiple different FGF receptors (Ornitz and Itoh, 2015), and previous work had shown considerable redundancy in FGF receptor action in control of lens fiber development (Lovicu and Overbeek, 1998; Zhao et al., 2008), we hypothesized that selectively activating the expression of any individual FGF in *Lhx2*-deficient retina might rescue lens development. We accomplished this by using *pMes-Fgf10* transgenic mice, a previously described line in which Cre-dependent excision of a

transcriptional stop cassette leads to expression of full-length mouse *Fgf10* under the control of the chick *β-actin* promoter (Song et al., 2013). Using this line, we aimed to selectively induce *Fgf10* expression in neuroretina of both control and *Chx10-Cre;Lhx2$^{lox/lox}$* mice (Fig. 3 *B* and *D*). We confirmed that *Fgf10* expression could be robustly and selectively induced in neuroretina of E13.5 *Chx10-Cre;Lhx2$^{lox/+}$;pMes-Fgf10* as well as *Chx10-Cre;Lhx2$^{lox/lox}$;pMes-Fgf10* mice (Fig. S2*A* and 3 *F* and *H*). Furthermore, we observed that FGF target genes, *Etv5*, *Etv1* and *Spry2*, were substantially upregulated in lenses of *Chx10-Cre;Lhx2$^{lox/+}$;pMes-Fgf10* mice relative to *Chx10-Cre;Lhx2$^{lox/+}$* controls (Fig. 3). Strikingly, we also observed robust induction of these same FGF target genes in the lenses of *Chx10-Cre;Lhx2$^{lox/lox}$;pMes-Fgf10* mice relative to *Chx10-Cre;Lhx2$^{lox/lox}$* mutants (Fig. 3). By E17.5, *Fgf10* expression in *Chx10-Cre;Lhx2$^{lox/+}$;pMes-Fgf10* mice was absent from central retinal, and became restricted to a small subset of cells at the neuroretinal periphery (Fig. S3*C*). In contrast, *Fgf10* expression was still seen in *Chx10-Cre;Lhx2$^{lox/lox}$;pMes-Fgf10* mice at both E17.5 and P0.5 (Fig. S3 *E* and *J*).

Retinal overexpression of Fgf10 leads to the persistence of lens stalk

Overexpression of *Fgf10* on a control background did not lead to any gross defects in lens development. The morphology and marker expression of *Chx10-Cre;Lhx2$^{lox/+}$;pMes-Fgf10* lenses were comparable to those of *Chx10-Cre;Lhx2$^{lox/+}$* controls (Fig. 4, 5 and S5). However, *Chx10-Cre;Lhx2$^{lox/+}$;pMes-Fgf10* lenses were slightly but significantly larger than control lenses at all time points examined (Fig. S2*B*). In addition, the anterior pole of the lens remained tethered to the surface ectoderm (Fig. S4 *B*, *D*, *F* and *H*) and this persistent lens stalk led to the development of corneal opacification in some adult mice (Fig. S4*J*).

Forced expression of FGF10 in Lhx2-deficient neuroretina rescues lens fiber differentiation

To investigate whether restoration of retinal FGF expression was able to rescue lens development in Lhx2 knockout animals, we conducted a detailed characterization of the expression of lens markers at multiple time points. At E11.5, prior to the formation of distinct lens fiber cells, no clear difference in lens size or the expression of Prox1 or β-crystallin was observed among *Chx10-Cre;Lhx2$^{lox/+}$*, *Chx10-Cre;Lhx2$^{lox/lox}$* and *Chx10-Cre;Lhx2$^{lox/lox}$;pMes-Fgf10* mice (Fig. S2*B* and 4 *A* – *D*). This may reflect that fact that Lhx2 deletion from neuroretina is not complete until E11.5, thus allowing lens development to proceed normally prior to this point. However by E12.5, after the onset of lens fiber differentiation, a dramatic reduction in lens size was seen in both *Chx10-Cre;Lhx2$^{lox/lox}$* and *Chx10-Cre;Lhx2$^{lox/lox}$;pMes-Fgf10* relative to *Chx10-Cre;Lhx2$^{lox/+}$* mice (Fig. S2*B*). However, lens size in *Chx10-Cre;Lhx2$^{lox/lox}$;pMes-Fgf10* mice was significantly larger than that of *Chx10-Cre;Lhx2$^{lox/lox}$* mice, with Prox1-positive differentiating lens fiber cells observed only in *Chx10-Cre;Lhx2$^{lox/lox}$;pMes-Fgf10* lenses (Fig. 4 *G* and *H*). This difference in lens size and lens fiber differentiation became more prominent as development proceeded. By E15.5, *Chx10-Cre;Lhx2$^{lox/lox}$;pMes-Fgf10* mice showed well-defined lenses filled with β-crystallin positive lens fiber cells (Fig. 4*P*). By P0.5, more than half of all *Chx10-Cre;Lhx2$^{lox/lox}$* mice no longer had a visible lens rudiment. When a lens rudiment was detectable, it was extremely small (Fig. 4*W* and S2*B*). However, all *Chx10-Cre;Lhx2$^{lox/lox}$;pMes-Fgf10* mice examined at P0.5 showed well-defined, though often small, lenses that expressed Prox1 and β-crystallin. Comparisons of eyes for the presence or absence of lenses in *Chx10-Cre;Lhx2$^{lox/lox}$* and *Chx10-Cre;Lhx2$^{lox/lox}$;pMes-Fgf10* mice at P0.5 indicated that the maintenance of lenses from FGF10 overexpression in *Chx10-Cre;Lhx2$^{lox/lox}$;pMes-Fgf10* mice was statistically significant (Fig. S2*C*). Interestingly, at no point did overexpression of *Fgf10* rescue defects in neuroretinal size (Fig. S2*D*). Expression

of β-crystallin in lens epithelial cells through P0.5 was observed in lens epithelial cells of both *Chx10-Cre;Lhx2*$^{lox/lox}$ and *Chx10-Cre;Lhx2*$^{lox/lox}$*;pMes-Fgf10* mice (Fig. 4 *G*,*H*,*K*,*P*,*T*,*X*). In contrast, β-crystallin expression was restricted to lens fiber cells in *Chx10-Cre;Lhx2*$^{lox/+}$ controls and *Chx10-Cre;Lhx2*$^{lox/lox}$*;pMes-Fgf10* by E12.5 (Fig. 4 *E*,*F*).

To further characterize the rescue of lens development observed following neuroretinal-specific overexpression of *Fgf10* in *Lhx2*-deficient mice, we analyzed the expression of additional lens markers, a selective marker for lens epithelial cells, E-cadherin, and two markers for lens fiber cells, N-cadherin and Aquaporin0 (originally known as main intrinsic polypeptide, MIP) (Xu et al., 2002; Yancey et al., 1988). We observed that *Chx10-Cre;Lhx2*$^{lox/lox}$ animals initially formed E-cadherin-positive lens vesicle but failed to differentiate to form lens fiber cells that are positive for N-cadherin or Aquaporin0 at E12.5 (Fig. S5*G* and 5*G*). As development progressed, these E-cadherin-positive lens vesicles got smaller and were no longer detectable in most animals by E18.5 (Fig. S5*S*). In contrast, *Chx10-Cre;Lhx2*$^{lox/lox}$*;pMes-Fgf10* mice continued to robustly express E-cadherin at E13.5, and begin to show a progressive increase in N-cadherin expression from this point through P0.5 (Fig. S5 *L*, *P*, *T* and *X*). We also observed that by E15.5 *Chx10-Cre;Lhx2*$^{lox/lox}$*;pMes-Fgf10* mice showed robust expression of Aquaporin0, a mature lens fiber cell marker, although the onset of Aquaporin0 expression was delayed relative to controls (Fig. 5). However, the *Chx10-Cre;Lhx2*$^{lox/lox}$*;pMes-Fgf10* rescue lens failed to develop normal lens polarity. E-cadherin and Prox1-positive cells persisted in the posterior pole of the lens at all time points examined (Fig. 4, 5 and S5).

FGF10 overexpression in Lhx2-deficient neuroretina promotes lens cell proliferation and survival

Exogenous FGFs have been reported to both promote the proliferation and survival of lens epithelial cells, in addition to driving lens fiber cell differentiation. To determine whether lens epithelial cell proliferation and survival were altered by overexpression of *Fgf10*, we examined the expression of Ki67 and activated caspase-3 (c-caspase 3), respectively, at E12.5 (Fig. 6). We observed a significant increase in lens epithelial cell proliferation in *Chx10-Cre;Lhx2*$^{lox/lox}$*;pMes-Fgf10* relative to *Chx10-Cre;Lhx2*$^{lox/lox}$ mutant lens (Fig. 6*E*). Cell death was increased in both *Chx10-Cre;Lhx2*$^{lox/lox}$ mutants and *Chx10-Cre;Lhx2*$^{lox/lox}$*;pMes-Fgf10* rescue mice relative to the *Chx10-Cre;Lhx2*$^{lox/+}$ and *Chx10-Cre;Lhx2*$^{lox/+}$*;pMes-Fgf10* controls, but was decreased in rescue mice relative to mutants (Fig. 6*F*). We thus conclude that overexpression of *Fgf10* in *Lhx2*-deficient neuroretina promotes lens cell proliferation, survival and differentiation.

Loss of Lhx2 expression in neuroretina also disrupts BMP signaling in the lens

A previous study has shown that Lhx2 regulates lens placode formation through BMP signaling (Yun et al., 2009), while other studies have shown an essential role of BMP signaling in lens induction as well as fiber differentiation (Boswell et al., 2008; Furuta and Hogan, 1998; Jarrin et al., 2012; Murali et al., 2005; Wawersik et al., 1999). To investigate whether BMP signaling was altered in either *Lhx2*-deficient or *Fgf10*-overexpressing eyes, we performed *in situ* hybridization for *Bmp4* and *Bmp7*, and immunostaining for phosphorylated SMAD1, 5 and 9 (pSmad1/5/9) at E13.5 (Fig. 7). In both *Chx10-Cre;Lhx2*$^{lox/+}$ and *Chx10-Cre;Lhx2*$^{lox/+}$*;pMes-Fgf10* controls, broad *Bmp4* expression was observed in neuroretina, RPE, and lens epithelial and differentiating fiber cells while more restricted *Bmp7* expression was detected in a subset of neuroretinal cells, RPE and lens epithelial cells (Fig. 7 *A*, *B*, *E* and *F*). Loss of neuroretinal Lhx2 expression led to a dramatic reduction of *Bmp4* expression in *Chx10-Cre;Lhx2*$^{lox/lox}$ mutant neuroretina and lens, while forced *Fgf10* expression partially rescued *Bmp4* expression in *Chx10-Cre;Lhx2*$^{lox/lox}$*;pMes-*

Fgf10 neuroretina and lens (Figure 7 *C* and *D*). *Bmp7* expression was not altered in both *Chx10-Cre;Lhx2*$^{lox/lox}$ mutants and *Chx10-Cre;Lhx2*$^{lox/lox}$*;pMes-Fgf10* rescue mice in agreement with a previous study by Hägglund et al. (2011) (Figure 7 *G* and *H*). Robust pSmad1/5/9 expression was observed in the neuroretina of both *Chx10-Cre;Lhx2*$^{lox/+}$ and *Chx10-Cre;Lhx2*$^{lox/+}$*;pMes-Fgf10* controls in the dorsoventral gradient. The expression was also observed in the nuclei of differentiating lens fiber cells (Fig. 7 *M* and *N*). In contrast, even though some pSmad1/5/9 staining was observed the neuroretina of both *Chx10-Cre;Lhx2*$^{lox/lox}$ and *Chx10-Cre;Lhx2*$^{lox/lox}$*;pMes-Fgf10* animals, pSmad1/5/9 expression was not detected in the lens of both lines (Figure 7 *O*, *P*). We conclude that loss of neuroretinal Lhx2 disrupts *Bmp4* expression and severely reduces BMP signaling in the lens.

Discussion

In this study, we showed that Lhx2 regulated the expression of *Bmp4* and multiple FGF genes – *Fgf3, Fgf9* and *Fgf15* – in neuroretina during early stages of retinal neurogenesis. The downregulation of these retinal-derived FGFs in Lhx2 knockout animals contributed to severe defects in lens cell proliferation, survival and differentiation. Restoring FGF expression in neuroretina, however, led to a partial rescue of lens development defects, despite continued retinal development defects. These findings demonstrate the central role of Lhx2 in regulating lens development, and strongly suggest that FGFs do indeed comprise a major component of the long-sought retinal-derived signals that controls lens maturation.

Previous work has shown that Lhx2 expression in the optic neuroepithelium is essential for lens placode specification (Yun et al., 2009). Our findings demonstrate the continued requirement of Lhx2 in the neuroretina past lens vesicle formation in regulating lens cell proliferation, survival and differentiation. The present study examined later stages of lens development than this earlier work, and identified a number of key differences in the relative contribution of BMP and FGF signaling. The previous study showed that loss of Lhx2 from optic vesicle severely disrupted *Bmp4/7* expression, but only modestly reduced FGF signaling, as evidenced by continued expression of *Fgf8*, *Erm (Etv5)* and phosphorylated ERK1/2 (pERK) in the optic vesicle and surface ectoderm. This same study showed that adding BMP7 or the combination of BMP4 and BMP7 to *Lhx2*$^{-/-}$ head culture was sufficient to induce Sox2 expression in surface ectoderm (Yun et al., 2009). Other studies have also demonstrated an essential role for BMP4/7 signaling in early stages of lens development (Furuta and Hogan, 1998; Murali et al., 2005; Pandit et al., 2015; Wawersik et al., 1999). In contrast, our study indicated FGF signaling as perhaps the major mediator in Lhx2 regulation of lens maturation. Loss of neuroretinal Lhx2 led to reduced retinal *Bmp4* expression, and severely disrupted BMP signaling in the lens, and these changes were not rescued by overexpression of *Fgf10* (Figure 7). Nonetheless, lens fiber development was substantially, though not completely, rescued, suggesting that this process is at least partially independent of BMP signaling. This difference in the relative contribution of FGF and BMP signaling may reflect differences in the roles of neuroretina-derived BMP and FGF signaling during earlier and later stages of lens development. However, the lack of complete rescue may thus result from the well-documented synergistic role of BMP and FGF signaling in promoting lens fiber differentiation (Boswell et al., 2008; Boswell and Musil, 2015; Jarrin et al., 2012). The extent to which restoring BMP signaling can rescue lens development in *Lhx2*-deficient mice awaits further investigation.

Our finding that Lhx2 regulates neuroretinal FGFs is supported by a previous study from our lab that showed direct binding of Lhx2 to *cis*-regulatory regions of *Fgf15* in neonatal mouse retina (de Melo et al., 2016). Although neuroretina-specific loss of function of other retinal progenitor-expressed transcription factors disrupts retinal progenitor cell proliferation and differentiation, and leads to microphthalmia (Burmeister et al., 1996;

Marquardt et al., 2001; Taranova et al., 2006), only loss of *Lhx2* significantly disrupts lens development. It is likely that these other mutant lines maintain neuroretinal expression of one or more FGFs, leading to normal lens development even in the face of a hypoplastic neuroretina.

Previous cell culture-based studies demonstrate that FGF signaling regulates multiple aspects of lens cell development and maturation (McAvoy and Chamberlain, 1989; Schulz et al., 1993). This study provides *in vivo* evidence for the importance of FGF signaling in lens cell proliferation, survival and differentiation. Our findings identify FGF3, 9 and 15 as the three neuroretinal-derived FGFs that regulate lens development. Previous studies show that FGF3 can activate FGFR2b and 1b; FGF9 can activate FGFR3c, 2c, 1c, 3b and 4; and FGF15 can activate FGFR1c, 2c, 3c and 4 (Ornitz et al., 1996; Zhang et al., 2006). Neuroretinal expression of these three different FGFs, each of which can activate different subsets of FGF receptors, likely accounts for the observation that only *Fgfr1/2/3* triple mutants produced severe defects in lens development (Zhao et al., 2008). This also likely accounts for the failure thus far to observe defects in lens fiber development in individual or pairwise combinations of targeted *Fgf* mutations (Robinson, 2006). Our ability to rescue lens fiber development by overexpression of *Fgf10*, which is expressed only at low levels in developing retina, agrees with previous findings of redundant roles of FGF3 and FGF10 in regulating cardiovascular and inner ear development (Alvarez et al., 2003; Urness et al., 2011).

Retinal overexpression of *Fgf10* in animals that are not deficient for Lhx2 leads to the persistent close apposition of lens and surface ectoderm at the anterior lens pole (Fig. S3). This phenotype was also observed in a number of other mutant mouse lines, including a transgenic mouse line that expressed a dominant negative FGF receptor in the presumptive lens ectoderm (Faber et al., 2001; Wolf et al., 2009; Zhao et al., 2012). It is possible that a tightly controlled level of FGF signaling activities is required for the lens vesicle to detach completely from the surface ectoderm. Alternatively, the spatial expression pattern of FGFs in neuroretina might influence lens vesicle detachment. At E13.5 when lens vesicle detachment from the surface ectoderm is complete, *Fgf3*, *9* and *15* are all predominantly expressed in central but not peripheral retina (Fig. 2). In contrast, *Fgf10* at this stage is expressed across the whole retina in *Chx10-Cre;Lhx2*$^{lox/+}$*;pMes-Fgf10* animals (Fig. 3), and Fgf10 secretion from peripheral retina may interfere with the complete detachment of the lens vesicle.

The rescue of lens development that we observe following *Fgf10* overexpression is incomplete, with lenses being quite small and lacking normal anterior-posterior polarity (Fig. 4, S3 and S4). Moreover, lens differentiation is delayed, as seen by the persistent co-expression of beta-crystallin and E-cadherin in lens epithelial cells (Fig. 4) and the delayed onset of Aqp0 expression in lens fiber cells (Fig. 5). Several factors may account for this lack of complete rescue. First, the retina remains very small and severely disorganized. These persistent defects may physically limit lens growth. Furthermore, in normal eyes, different regions of the lens are exposed to different ocular environments, with the anterior part of the lens bathed in aqueous humor while the posterior part in vitreous humor. As suggested by previous studies (Chamberlain and McAvoy, 1997), this distinct ocular architecture allows different parts of the lens to be exposed to different levels of FGFs, promoting the establishment of lens polarity. However, all regions of our rescued lenses were likely exposed to similar concentrations of FGF10. Since FGFs show dose-dependent effects on proliferation of lens epithelial cells and their differentiation into lens fiber cells (McAvoy and Chamberlain, 1989; Schulz et al., 1993), the disruption of the normal gradient of FGF signaling in our rescue animals likely accounts for the persistence of lens epithelial cells at the posterior pole. In addition, as mentioned above, overexpression of *Fgf10* in neuroretina

did not rescue BMP signaling in the lens in *Lhx2*-deficient eyes. A schematic figure summarizing our results is shown in Figure 6*G*.

Materials and Methods

Animals: *Lhx2*$^{lox/lox}$ (Mangale et al., 2008) mice were obtained from Dr. Edwin Monuki (University of California, Irvine). *Chx10-Cre* (Rowan and Cepko, 2004) mice were a gift from Dr. Connie Cepko (Harvard). *pMes-Fgf10* (Song et al., 2013) mice were generously provided by Dr. Yang Chai (University of Southern California). *Ai9 (R26-CAG-lox-stop-lox-tdTomato)* (Madisen et al., 2010) mice were a gift from Dr. Xinzhong Dong (Johns Hopkins). *Chx10-Cre;Lhx2*$^{lox/+}$, *Chx10-Cre;Lhx2*$^{lox/+}$*;pMes-Fgf10*, *Chx10-Cre;Lhx2*$^{lox/lox}$, *Chx10-Cre;Lhx2*$^{lox/lox}$*;pMes-Fgf10* and *Chx10-Cre;Ai9* mice were generated by breeding with subsequent backcrossing. Immunohistochemistry or *in situ* hybridization was performed to confirm Cre-mediated inactivation of Lhx2. Only animals with successful inactivation of Lhx2 expression were included in the analysis. All experimental animal procedures were preapproved by the Johns Hopkins University Institutional Animal Care and Use Committee.

Quantitative RT-PCR: The cDNAs of E13.5 dissected retinas were synthesized from total RNAs using SuperScript III First-Strand Synthesis System (Invitrogen). Quantitative RT-PCR was performed using Brilliant III Ultra-Fast SYBR Green QPCR Master Mix (Agilent) on a 7300 Real-Time PCR System (Applied Biosystems) following the manufacturers' recommended protocols. Primer sets for genes examined were as follows: fibroblast growth factor 3 (*Fgf3*) forward – TGCGCTACCAAGTACCACC, *Fgf3* reverse – CACCGCAGTAATCTCCAGGAT; *Fgf9* forward – ATGGCTCCCTTAGGTGAAGTT, *Fgf9* reverse – TCCGCCTGAGAATCCCCTTT; *Fgf10* forward – GCAGGCAAATGTATGTGGCAT, *Fgf10* reverse – ATGTTTGGATCGTCATGGGGA; *Fgf15* forward – GGTCCCTATGTCTCCAACTGC, *Fgf15* reverse – CTTGATGGCAATCGTCTTCAGA; *Gapdh* forward – AGGTCGGTGTGAACGGATTTG, *Gapdh* reverse – TGTAGACCATGTAGTTGAGGTCA.

***In situ* Hybridization**: Chromogenic *in situ* hybridization experiments were performed as described previously with minor changes (Blackshaw et al., 2004). Briefly, fresh frozen sections were fixed by 4% paraformaldehyde and hybridized with digoxigenin-labeled probes at 70°C overnight. Excess probes were washed out, followed by rinsing in RNase buffer (0.5M NaCl, 10mM Tris pH 7.5, 5mM EDTA) at 37°C and treatment with RNaseA diluted in RNase buffer to 2ug/ml for 30 minutes at 37°C. Slides were then washed in RNase buffer, and .2X SSC prior to being blocked with sheep serum and overnight incubation in anti-digoxigenin antibodies conjugated to alkaline phosphatase (1:5000) at 4°C. Color was developed with combinations of the chromogens nitroblue tetrazolium (NBT) and 5-bromo, 4-chloro, 3-indolylphosphate (BCIP). *Fgf3*, *Fgf9* and *Fgf10* constructs were obtained from Marysia Placzek (University of Sheffield). *Bmp4* and *Bmp7* probes were obtained from Dr. Jane Dodd (Columbia University) and Dr. Jeanette C. Perron (St. John's University). RNA probes were generated using the following EST sequences as templates: *Etv5* (GenBank accession #BE996421), *Etv1* (GenBank accession #AI852622), *Spry2* (GenBank accession #BC095983) and *Fgf15* (GenBank accession #BE952015). *Lhx2* probe template was amplified from retinal cDNA. The sequences of the primers used for amplification were forward – ACCATGCCGTCCATCAGC and reverse – GGCGTTGTAAGCTGCCAG.

Histology and Immunohistochemistry: Haematoxylin and eosin (H+E) staining and fluorescence immunohistochemistry were performed as previously described (de Melo et al., 2012; Roy et al., 2013). The following primary antibodies were used: rabbit anti-Lhx2 (1:1,000; generated for our lab by Covance (de Melo et al., 2012)), mouse anti-Pax6 (1:200; DSHB), rabbit anti-β-crystallin (1:500; generous gift from Dr. Jeremy Nathans), mouse anti-Prox1 (1:200; MAB5654, Millipore), rabbit anti-E-Cadherin (1:200; 3195, Cell Signaling), mouse anti-N-Cadherin (1:200; 333900, Novex), rabbit anti-Aquaporin 0 (1:200; AB3071, Millipore), rabbit anti-Cleaved Caspase-3 (1:200; 9664, Cell Signaling), mouse anti-Ki67 (1:200; 550609 (Clone B56), BD Pharmingen), rat anti-RFP (1:1000; ABIN334653, Chromotek) and rabbit anti-pSmad1/5/9 (1:300; 13820, Cell Signaling). Secondary antibodies used were as follows: FITC-conjugated donkey anti-mouse IgG (1:500; 715-095-150, Jackson ImmunoResearch), Alexa Fluor 488-conjugated goat anti-mouse IgG, Fcγ subclass 1 specific (1:500; 115-545-205, Jackson ImmunoResearch), FITC-conjugated goat anti-mouse IgG (subclasses 1+2a+2b+3), Fcγ fragment (1:500; 115-095-164, Jackson ImmunoResearch), Alexa Fluor 594-conjugated donkey anti-rabbit IgG (1:500; 711-585-152, Jackson ImmunoResearch), and Alexa Fluor 555-conjugated goat anti-rat IgG (1:500; A-21434, Invitrogen). H+E sections were imaged using a Zeiss Axioskop 2 Mot Plus Microscope. Immunohistochemical sections were imaged on a Zeiss Meta 510 LSM confocal microscope.

Cell quantification: The total number of DAPI-, Ki67- and c-Caspase-3-positive cells on each lens section was quantified and the percentage of Ki67- and c-Caspase-3-positive cells was calculated (n = 6 for *Chx10-Cre;Lhx2*$^{lox/+}$ and *Chx10-Cre;Lhx2*$^{lox/+}$*;pMes-Fgf10*; n = 18 for *Chx10-Cre;Lhx2*$^{lox/lox}$ and *Chx10-Cre;Lhx2*$^{lox/lox}$*;pMes-Fgf10*). Lens and retinal sizes were measured using ImageJ ($n \geq 4$ for E11.5; $n \geq 9$ for E12.5; $n \geq 6$ for E13.5; $n \geq 7$ for P0.5.) All cell counts and measurements were repeated by a blinded student researcher.

Statistical Analysis: Data were presented as mean ± SEM. Statistical analysis was performed using GraphPad Prism Software. Comparisons of means between two groups were evaluated by Student's t-test. Comparison of means among multiple groups was performed by one-way ANOVA followed by Tukey's and Sidak's multiple comparison tests. Categorical data was analyzed using Fisher's exact test. $P < 0.05$ was considered to be statistically significant.

Acknowledgements: This works was supported by NIH R01EY020560 and R01EY017015 (to S.B), a grant from the Knights Templar Pediatric Ophthalmology Foundation (J.d.M), and NIH F32EY024201 (to B.S.C). S.B. was a W.M. Keck Distinguished Young Scholar in Medical Research. The authors declare no competing financial interests. We thank Dr. Marysia Placzek for *Fgf3*, *Fgf9* and *Fgf10* probes; Drs. Carol Mason and Jeanette Perron for *Bmp4* and *Bmp7* probes; and Dr. Yang Chai for pMes-Fgf10 transgenic mouse line,

Figures

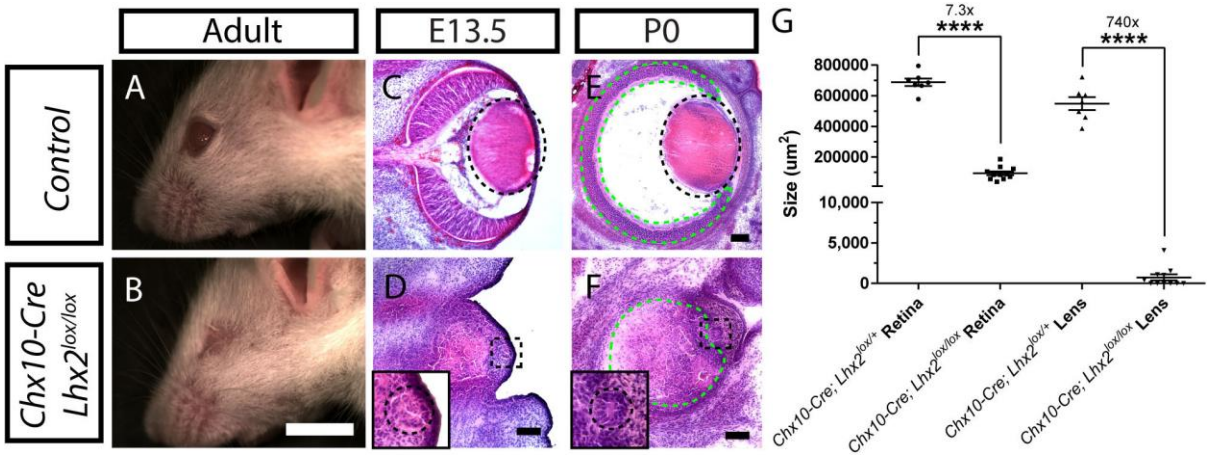

Figure 1: Loss of function of Lhx2 in neuroretina led to microphthalmia and lens development defects. (A – B) Lateral view of Control (A) and *Chx10-Cre;Lhx2*$^{lox/lox}$ animals (B) indicating microphthalmia in *Chx10-Cre;Lhx2*$^{lox/lox}$ animals. (C – F) H+E staining of eye sections from E13.5 (C, D) and P0.5 (E, F) of Control (C, E) and *Chx10-Cre;Lhx2*$^{lox/lox}$ (D, F) mice. Dotted green and black outlines mark the retinas and lenses, respectively (C – F) and insets (D, F) are digital zooms of the outlined regions. (G) Graph indicating average neuroretinal area and lens area in sections of control and *Chx10-Cre;Lhx2*$^{lox/lox}$ mice at P0.5. (Unpaired two-tailed t-test; n = 7 for *Chx10-Cre;Lhx2*$^{lox/+}$; n = 11 for *Chx10-Cre;Lhx2*$^{lox/lox}$; ****P<0.0001) (Scale Bars: 5 mm (A, B), 100 µm (C – F))

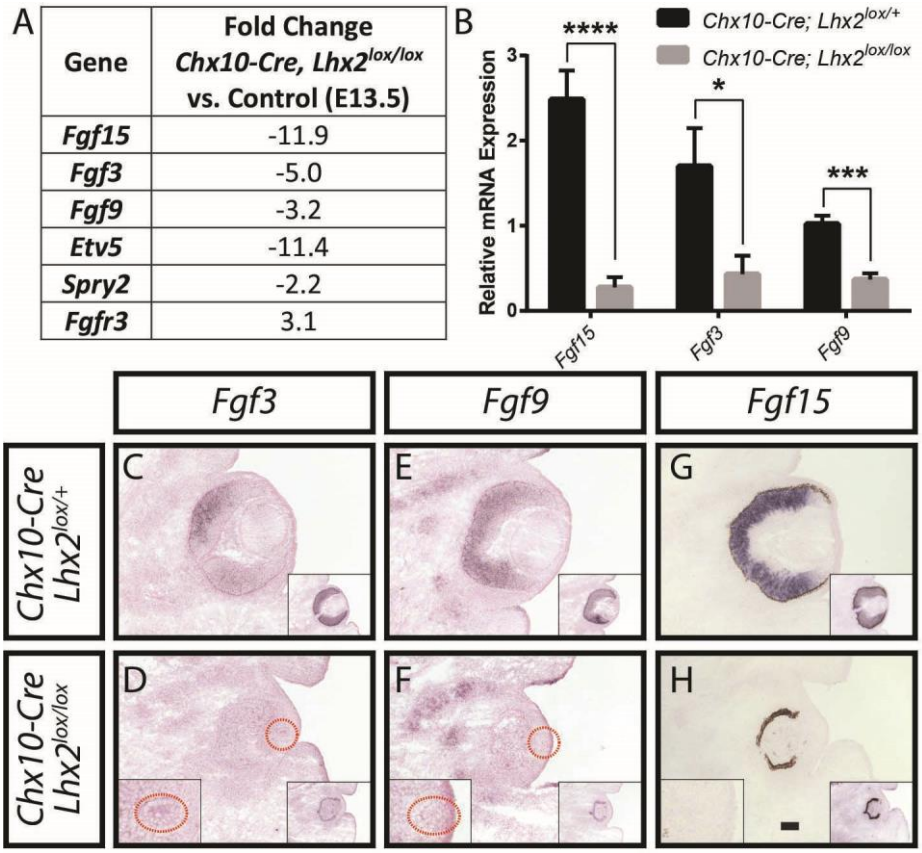

Figure 2: *Fgf3, Fgf9* and *Fgf15* were downregulated in *Chx10-Cre;Lhx2*$^{lox/lox}$ retinas. (A) Table indicating *Fgfs* and FGF-regulated genes expression from microarray analysis of E13.5 control and *Chx10-Cre;Lhx2*$^{lox/lox}$ retinas. (B) Real-time quantitative PCR analysis of *Fgf3*, *Fgf9* and *Fgf15* mRNA expression levels in *Chx10-Cre;Lhx2*$^{lox/lox}$ retinas compared to *Chx10-Cre;Lhx2*$^{lox/+}$ controls at E13.5. Data represent mean normalized to *Gapdh* values ± SEM. (Unpaired two-tailed t-test; n=3; *P<0.05; ***P<0.001; ****P<0.0001) (C – H) *In situ* hybridization of *Fgf3*, *Fgf9* and *Fgf15* mRNA expression levels in *Chx10-Cre;Lhx2*$^{lox/+}$ (C, E and G) and *Chx10-Cre;Lhx2*$^{lox/lox}$ (D, F and H) eyes at E13.5. Dotted red circles mark the lenses with zoomed-in images of the lenses included in left insets (D and F). Lens *Lhx2* expression in adjacent sections is shown in right insets. *Lhx2* expression in RPE is maintained and outlines the neural retina in unpigmented animals (right insets in D and F). (Scale Bars: 100 µm)

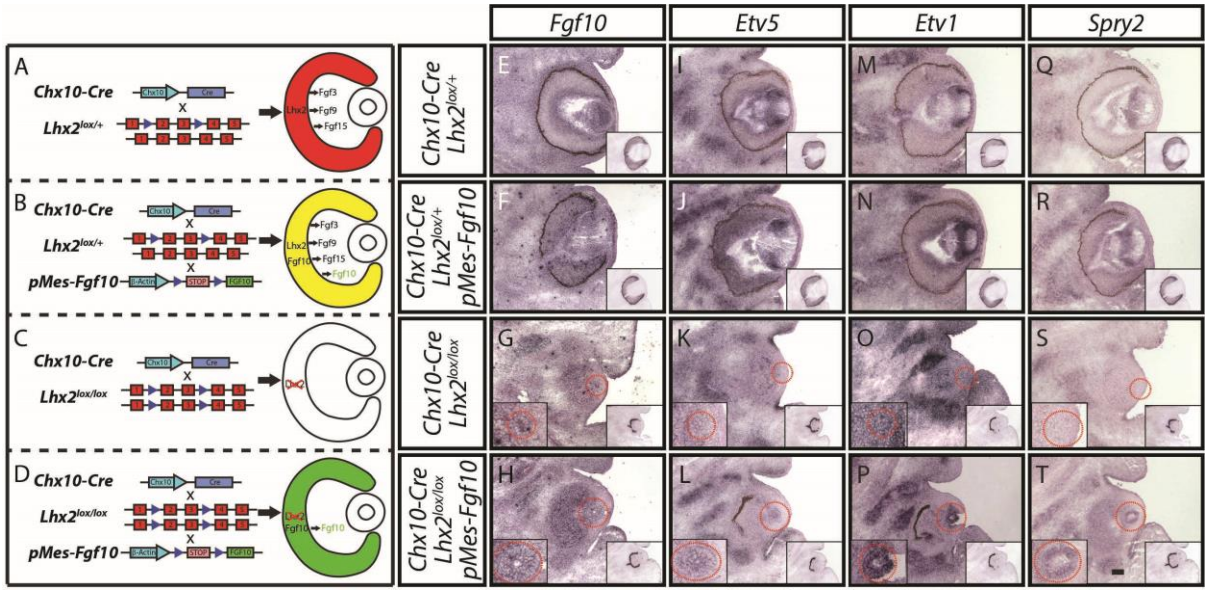

Figure 3: Cre-mediated induction of *Fgf10* expression in *Chx10-Cre;Lhx2$^{lox/lox}$;pMes-Fgf10* retinas restored expression of FGF-regulated genes in lens. (A – D) Schematic diagrams depicting the mouse genetics and anticipated retinal derived FGF expression for (A) *Chx10-Cre;Lhx2$^{lox/+}$*, (B) *Chx10-Cre;Lhx2$^{lox/+}$; pMes-Fgf10*, (C) *Chx10-Cre;Lhx2$^{lox/lox}$* and (D) *Chx10-Cre;Lhx2$^{lox/lox}$;pMes-Fgf10* eyes. (E – T) *In situ* hybridization demonstrates *Fgf10* induction in neuroretina (E – H), and induction of expression of FGF-regulated genes, including *Etv5* (I – L), *Etv1* (M – P), and *Spry2* (Q – T). Right insets indicate *Lhx2* expression in adjacent sections. *Lhx2* expression in RPE is maintained and outlines the neural retina in unpigmented animals (insets in G, K, O, S, H and T). Dotted red circles mark the lenses with zoomed-in images of the lenses included in left insets (G – T). (Scale Bars: 100 μm)

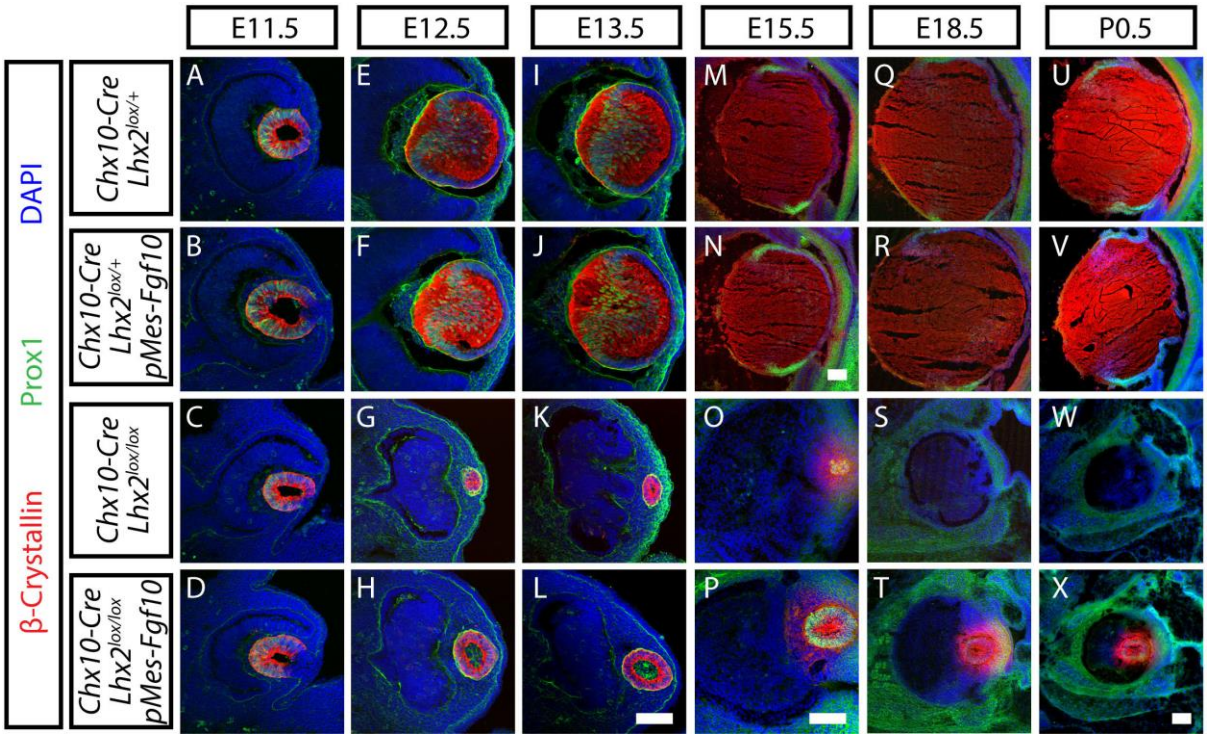

Figure 4: Overexpression of Fgf10 in *Chx10-Cre;Lhx2$^{lox/lox}$;pMes-Fgf10* animals rescued lens fiber development. Developmental time-course of immunohistochemical staining for Prox1 (green) and β-Crystallin (red) in lenses at E11.5 (A – D), E12.5 (E – H), E13.5 (I – L), E15.5 (M – P), E18.5 (Q – T) and P0.5 (U – X) of *Chx10-Cre;Lhx2$^{lox/+}$* (A, E, I, M, Q, U), *Chx10-Cre;Lhx2$^{lox/+}$;pMes-Fgf10* (B, F, J, N, R, V), *Chx10-Cre;Lhx2$^{lox/lox}$* (C, G, K, O, S, W) and *Chx10-Cre;Lhx2$^{lox/lox}$;pMes-Fgf10* animals (D, H, L, P, T, X). Nuclei are counter-stained with DAPI (blue). (Scale Bars: 100 µm)

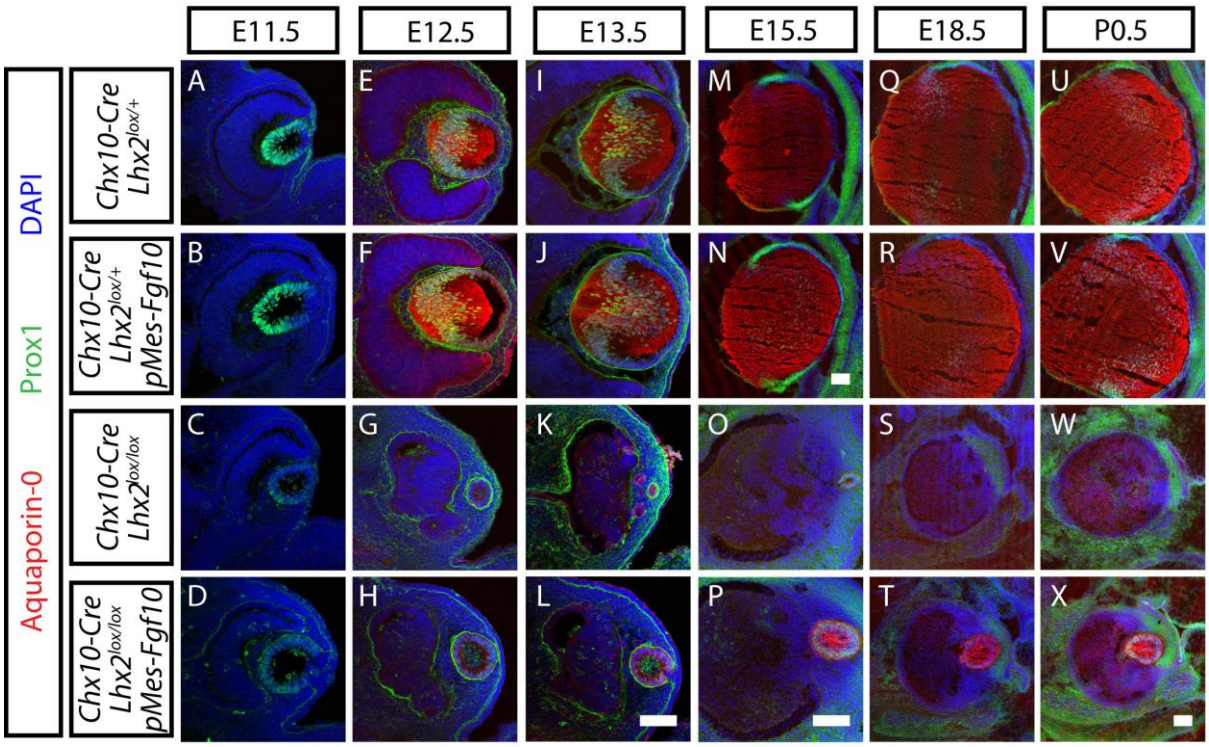

Figure 5: *Chx10-Cre;Lhx2$^{lox/lox}$;pMes-Fgf10* animals expressed the mature lens fiber marker Aquaporin-0. Developmental time-course of immunohistochemistry for Prox1 (green) and Aquaporin-0 (red) expression in lenses at E11.5 (A – D), E12.5 (E – H), E13.5 (I – L), E15.5 (M – P), E18.5 (Q – T) and P0.5 (U – X) of *Chx10-Cre;Lhx2$^{lox/+}$* (A, E, I, M, Q, U), *Chx10-Cre;Lhx2$^{lox/+}$;pMes-Fgf10* (B, F, J, N, R, V), *Chx10-Cre;Lhx2$^{lox/lox}$* (C, G, K, O, S, W) and *Chx10-Cre;Lhx2$^{lox/lox}$;pMes-Fgf10* animals (D, H, L, P, T, X). Nuclei are counter-stained with DAPI (blue). (Scale Bars: 100 μm)

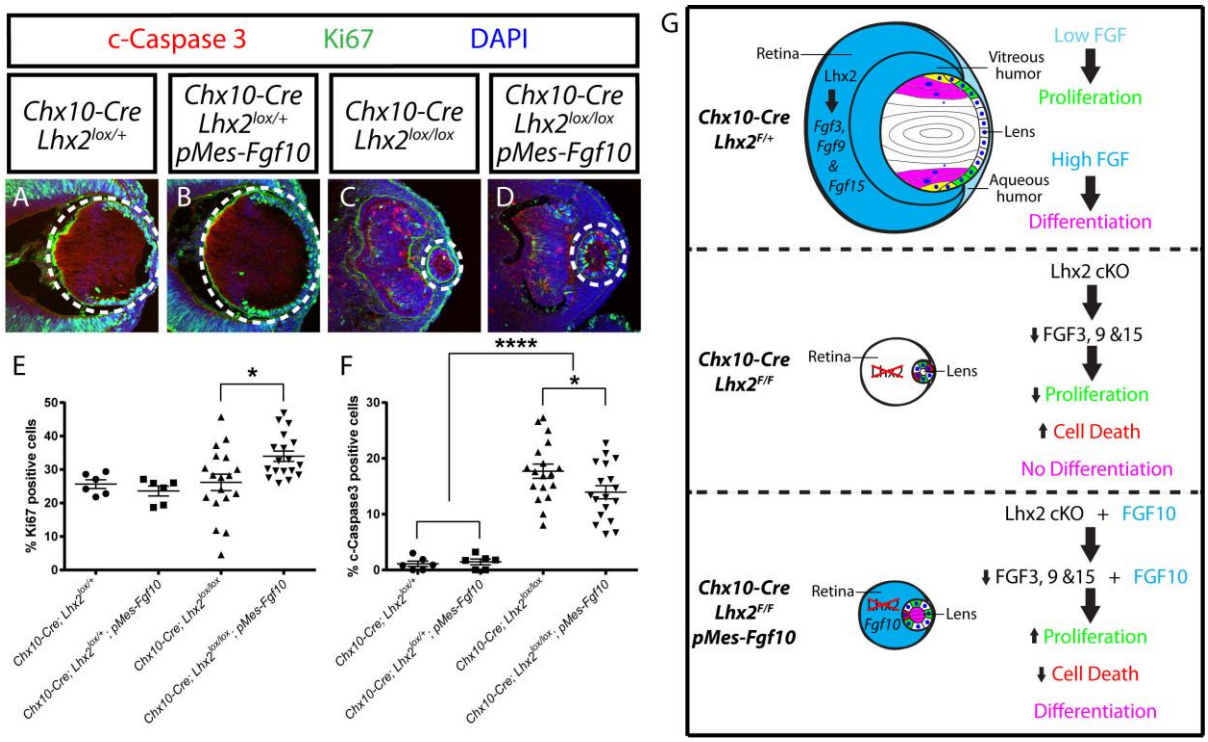

Figure 6: Fgf10 overexpression rescued defects in lens cell proliferation and cell death. (A – D) Immunostaining of E12.5 eye sections for Ki67 (green) and activated Caspase 3 (c-Caspase3, red). White dotted circles mark the lenses. (Scale Bars: 100 µm) (E) Graph indicating the percentage of Ki67-positive cells relative to all DAPI-positive cells in the lenses. (F) Graph indicating the percentage of c-Caspase3-positive cells over DAPI-positive cells in the lenses. (One-way ANOVA followed by Sidak's test; n = 6 for *Chx10-Cre;Lhx2*$^{lox/+}$ and *Chx10-Cre;Lhx2*$^{lox/+}$*;pMes-Fgf10*; n = 18 for *Chx10-Cre;Lhx2*$^{lox/lox}$ and *Chx10-Cre;Lhx2*$^{lox/lox}$*;pMes-Fgf10*, *P<0.05; ****P<0.0001; Error bars indicate SEM) (G) A graphical summary of the findings of this study.

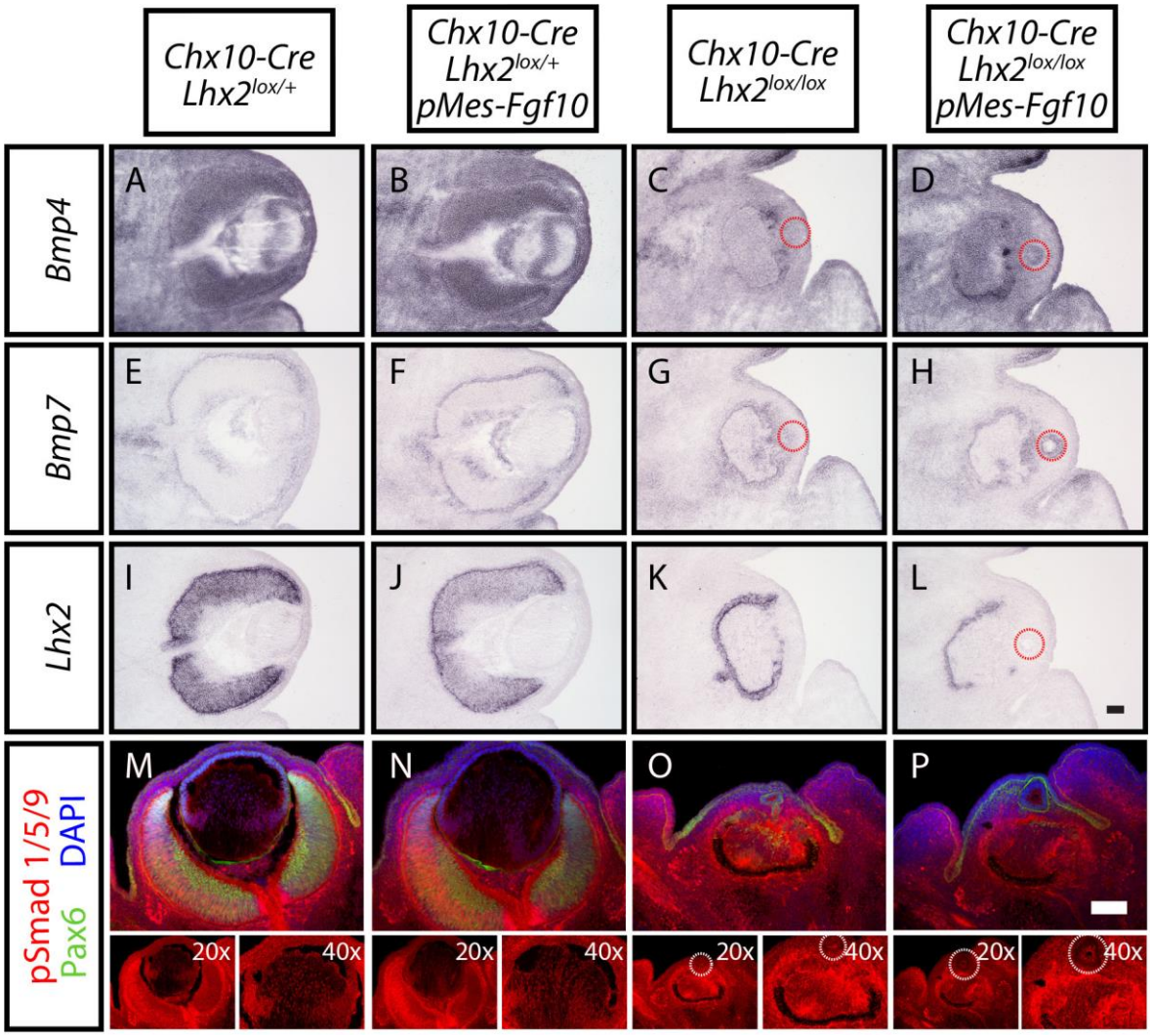

Figure 7: Selective deletion of Lhx2 in neuroretina led to downregulation of BMP signaling in the neuroretina and lens. (A – L) *In situ* hybridization of *Bmp4* (A – D), *Bmp7* (E – H) and *Lhx2* (I – L) mRNA expression levels in *Chx10-Cre;Lhx2*$^{lox/+}$ (A, E and I), *Chx10-Cre;Lhx2*$^{lox/+}$*; pMes-Fgf10* (B, F and J), *Chx10-Cre;Lhx2*$^{lox/lox}$ (C, G and K) and *Chx10-Cre;Lhx2*$^{lox/lox}$*;pMes-Fgf10* (D, H and L) eyes at E13.5. Dotted red circles mark the lenses (C, D G, H and L). (M – P) Immunohistochemical staining for Pax6 (green) and pSmad1/5/9 (red) in lenses of *Chx10-Cre;Lhx2*$^{lox/+}$ (M), *Chx10-Cre;Lhx2*$^{lox/+}$*;pMes-Fgf10* (N), *Chx10-Cre;Lhx2*$^{lox/lox}$ (O) and *Chx10-Cre;Lhx2*$^{lox/lox}$*;pMes-Fgf10* animals (P) at E13.5. Nuclei are counter-stained with DAPI (blue). The images of pSmad1/5/9 staining in single channel and higher magnification are included at the bottom. Dotted white circles mark the lenses (O and P). (Scale Bars: 100 µm)

References:

Alvarez, Y., Alonso, M.T., Vendrell, V., Zelarayan, L.C., Chamero, P., Theil, T., Bösl, M.R., Kato, S., Maconochie, M., Riethmacher, D., Schimmang, T., 2003. Requirements for FGF3 and FGF10 during inner ear formation. Dev. Camb. Engl. 130, 6329–6338. doi:10.1242/dev.00881

Blackshaw, S., Harpavat, S., Trimarchi, J., Cai, L., Huang, H., Kuo, W.P., Weber, G., Lee, K., Fraioli, R.E., Cho, S.-H., Yung, R., Asch, E., Ohno-Machado, L., Wong, W.H., Cepko, C.L., 2004. Genomic analysis of mouse retinal development. PLoS Biol. 2, E247. doi:10.1371/journal.pbio.0020247

Boswell, B.A., Musil, L.S., 2015. Synergistic interaction between the fibroblast growth factor and bone morphogenetic protein signaling pathways in lens cells. Mol. Biol. Cell 26, 2561–2572. doi:10.1091/mbc.E15-02-0117

Boswell, B.A., Overbeek, P.A., Musil, L.S., 2008. Essential Role of BMPs in FGF-Induced Secondary Lens Fiber Differentiation. Dev. Biol. 324, 202–212. doi:10.1016/j.ydbio.2008.09.003

Chamberlain, C.G., McAvoy, J.W., 1997. Fibre differentiation and polarity in the mammalian lens: a key role for FGF. Prog. Retin. Eye Res. 16, 443–478. doi:10.1016/S1350-9462(96)00034-1

Chamberlain, C.G., McAvoy, J.W., 1989. Induction of lens fibre differentiation by acidic and basic fibroblast growth factor (FGF). Growth Factors Chur Switz. 1, 125–134.

Chamberlain, C.G., McAvoy, J.W., 1987. Evidence that fibroblast growth factor promotes lens fibre differentiation. Curr. Eye Res. 6, 1165–1169.

Colvin, J.S., Feldman, B., Nadeau, J.H., Goldfarb, M., Ornitz, D.M., 1999. Genomic organization and embryonic expression of the mouse fibroblast growth factor 9 gene. Dev. Dyn. Off. Publ. Am. Assoc. Anat. 216, 72–88. doi:10.1002/(SICI)1097-0177(199909)216:1<72::AID-DVDY9>3.0.CO;2-9

Coulombre, J.L., Coulombre, A.J., 1963. Lens Development: Fiber Elongation and Lens Orientation. Science 142, 1489–1490. doi:10.1126/science.142.3598.1489

de Melo, J., Miki, K., Rattner, A., Smallwood, P., Zibetti, C., Hirokawa, K., Monuki, E.S., Campochiaro, P.A., Blackshaw, S., 2012. Injury-independent induction of reactive gliosis in retina by loss of function of the LIM homeodomain transcription factor Lhx2. Proc. Natl. Acad. Sci. U. S. A. 109, 4657–4662. doi:10.1073/pnas.1107488109

de Melo, J., Zibetti, C., Clark, B.S., Hwang, W., Miranda-Angulo, A. L., Qian, J., and Blackshaw, S., 2016. Lhx2 is an essential factor for retinal gliogenesis and Notch signaling. J. Neurosci 36, 2391-2405.

Faber, S.C., Dimanlig, P., Makarenkova, H.P., Shirke, S., Ko, K., Lang, R.A., 2001. Fgf receptor signaling plays a role in lens induction. Dev. Camb. Engl. 128, 4425–4438.

Furuta, Y., Hogan, B.L., 1998. BMP4 is essential for lens induction in the mouse embryo. Genes Dev. 12, 3764–3775.

Gunhaga, L., 2011. The lens: a classical model of embryonic induction providing new insights into cell determination in early development. Philos. Trans. R. Soc. B Biol. Sci. 366, 1193–1203. doi:10.1098/rstb.2010.0175

Hägglund, A.-C., Dahl, L., Carlsson, L., 2011. Lhx2 is required for patterning and expansion of a distinct progenitor cell population committed to eye development. PloS One 6, e23387. doi:10.1371/journal.pone.0023387

Jarrin, M., Pandit, T., Gunhaga, L., 2012. A balance of FGF and BMP signals regulates cell cycle exit and Equarin expression in lens cells. Mol. Biol. Cell 23, 3266–3274. doi:10.1091/mbc.E12-01-0075

Kurose, H., Bito, T., Adachi, T., Shimizu, M., Noji, S., Ohuchi, H., 2004. Expression of Fibroblast growth factor 19 (Fgf19) during chicken embryogenesis and eye development, compared with Fgf15 expression in the mouse. Gene Expr. Patterns GEP 4, 687–693. doi:10.1016/j.modgep.2004.04.005
Lovicu, F.J., McAvoy, J.W., 2005. Growth factor regulation of lens development. Dev. Biol. 280, 1–14. doi:10.1016/j.ydbio.2005.01.020
Lovicu, F.J., McAvoy, J.W., de Iongh, R.U., 2011. Understanding the role of growth factors in embryonic development: insights from the lens. Philos. Trans. R. Soc. Lond. B. Biol. Sci. 366, 1204–1218. doi:10.1098/rstb.2010.0339
Lovicu, F.J., Overbeek, P.A., 1998. Overlapping effects of different members of the FGF family on lens fiber differentiation in transgenic mice. Dev. Camb. Engl. 125, 3365–3377.
Lovicu, F.J., Robinson, M.L. (Eds.), 2004. Development of the Ocular Lens. Cambridge University Press.
Madisen, L., Zwingman, T.A., Sunkin, S.M., Oh, S.W., Zariwala, H.A., Gu, H., Ng, L.L., Palmiter, R.D., Hawrylycz, M.J., Jones, A.R., Lein, E.S., Zeng, H., 2010. A robust and high-throughput Cre reporting and characterization system for the whole mouse brain. Nat. Neurosci. 13, 133–140. doi:10.1038/nn.2467
Mangale, V.S., Hirokawa, K.E., Satyaki, P.R.V., Gokulchandran, N., Chikbire, S., Subramanian, L., Shetty, A.S., Martynoga, B., Paul, J., Mai, M.V., Li, Y., Flanagan, L.A., Tole, S., Monuki, E.S., 2008. Lhx2 selector activity specifies cortical identity and suppresses hippocampal organizer fate. Science 319, 304–309. doi:10.1126/science.1151695
McAvoy, J.W., Chamberlain, C.G., 1989. Fibroblast growth factor (FGF) induces different responses in lens epithelial cells depending on its concentration. Dev. Camb. Engl. 107, 221–228.
McAvoy, J.W., Chamberlain, C.G., de Longh, R.U., Hales, A.M., Lovicu, F.J., 1999. Lens development. Eye 13, 425–437. doi:10.1038/eye.1999.117
McAvoy, J.W., Fernon, V.T., 1984. Neural retinas promote cell division and fibre differentiation in lens epithelial explants. Curr. Eye Res. 3, 827–834.
Murali, D., Yoshikawa, S., Corrigan, R.R., Plas, D.J., Crair, M.C., Oliver, G., Lyons, K.M., Mishina, Y., Furuta, Y., 2005. Distinct developmental programs require different levels of Bmp signaling during mouse retinal development. Dev. Camb. Engl. 132, 913–923. doi:10.1242/dev.01673
Ornitz, D.M., Itoh, N., 2015. The Fibroblast Growth Factor signaling pathway. Wiley Interdiscip. Rev. Dev. Biol. 4, 215–266. doi:10.1002/wdev.176
Ornitz, D.M., Xu, J., Colvin, J.S., McEwen, D.G., MacArthur, C.A., Coulier, F., Gao, G., Goldfarb, M., 1996. Receptor specificity of the fibroblast growth factor family. J. Biol. Chem. 271, 15292–15297.
Pandit, T., Jidigam, V.K., Patthey, C., Gunhaga, L., 2015. Neural retina identity is specified by lens-derived BMP signals. Dev. Camb. Engl. 142, 1850–1859. doi:10.1242/dev.123653
Robinson, M.L., 2006. An essential role for FGF receptor signaling in lens development. Semin. Cell Dev. Biol. 17, 726–740. doi:10.1016/j.semcdb.2006.10.002
Rowan, S., Cepko, C.L., 2004. Genetic analysis of the homeodomain transcription factor Chx10 in the retina using a novel multifunctional BAC transgenic mouse reporter. Dev. Biol. 271, 388–402. doi:10.1016/j.ydbio.2004.03.039
Roy, A., de Melo, J., Chaturvedi, D., Thein, T., Cabrera-Socorro, A., Houart, C., Meyer, G., Blackshaw, S., Tole, S., 2013. Lhx2 is necessary for the maintenance of optic identity

and for the progression of optic morphogenesis. J. Neurosci. Off. J. Soc. Neurosci. 33, 6877–6884. doi:10.1523/JNEUROSCI.4216-12.2013
Schulz, M.W., Chamberlain, C.G., de Iongh, R.U., McAvoy, J.W., 1993. Acidic and basic FGF in ocular media and lens: implications for lens polarity and growth patterns. Dev. Camb. Engl. 118, 117–126.
Song, Z., Liu, C., Iwata, J., Gu, S., Suzuki, A., Sun, C., He, W., Shu, R., Li, L., Chai, Y., Chen, Y., 2013. Mice with Tak1 deficiency in neural crest lineage exhibit cleft palate associated with abnormal tongue development. J. Biol. Chem. 288, 10440–10450. doi:10.1074/jbc.M112.432286
Urness, L.D., Bleyl, S.B., Wright, T.J., Moon, A.M., Mansour, S.L., 2011. Redundant and dosage sensitive requirements for Fgf3 and Fgf10 in cardiovascular development. Dev. Biol. 356, 383–397. doi:10.1016/j.ydbio.2011.05.671
Wang, Q., McAvoy, J.W., Lovicu, F.J., 2010. Growth factor signaling in vitreous humor-induced lens fiber differentiation. Invest. Ophthalmol. Vis. Sci. 51, 3599–3610. doi:10.1167/iovs.09-4797
Wawersik, S., Purcell, P., Rauchman, M., Dudley, A.T., Robertson, E.J., Maas, R., 1999. BMP7 acts in murine lens placode development. Dev. Biol. 207, 176–188. doi:10.1006/dbio.1998.9153
Wilkinson, D.G., Bhatt, S., McMahon, A.P., 1989. Expression pattern of the FGF-related proto-oncogene int-2 suggests multiple roles in fetal development. Dev. Camb. Engl. 105, 131–136.
Wolf, L.V., Yang, Y., Wang, J., Xie, Q., Braunger, B., Tamm, E.R., Zavadil, J., Cvekl, A., 2009. Identification of pax6-dependent gene regulatory networks in the mouse lens. PloS One 4, e4159. doi:10.1371/journal.pone.0004159
Xu, L., Overbeek, P.A., Reneker, L.W., 2002. Systematic analysis of E-, N- and P-cadherin expression in mouse eye development. Exp. Eye Res. 74, 753–760.
Yamamoto, Y., 1976. Growth of Lens and Ocular Environment: Role of Neural Retina in the Growth of Mouse Lens as Revealed by an Implantation Experiment. Dev. Growth Differ. 18, 273–278. doi:10.1111/j.1440-169X.1976.00273.x
Yancey, S.B., Koh, K., Chung, J., Revel, J.P., 1988. Expression of the gene for main intrinsic polypeptide (MIP): separate spatial distributions of MIP and beta-crystallin gene transcripts in rat lens development. J. Cell Biol. 106, 705–714.
Yun, S., Saijoh, Y., Hirokawa, K.E., Kopinke, D., Murtaugh, L.C., Monuki, E.S., Levine, E.M., 2009. Lhx2 links the intrinsic and extrinsic factors that control optic cup formation. Dev. Camb. Engl. 136, 3895–3906. doi:10.1242/dev.041202
Zhang, X., Ibrahimi, O.A., Olsen, S.K., Umemori, H., Mohammadi, M., Ornitz, D.M., 2006. Receptor specificity of the fibroblast growth factor family. The complete mammalian FGF family. J. Biol. Chem. 281, 15694–15700. doi:10.1074/jbc.M601252200
Zhao, H., Yang, T., Madakashira, B.P., Thiels, C.A., Bechtle, C.A., Garcia, C.M., Zhang, H., Yu, K., Ornitz, D.M., Beebe, D.C., Robinson, M.L., 2008. Fibroblast growth factor receptor signaling is essential for lens fiber cell differentiation. Dev. Biol. 318, 276–288. doi:10.1016/j.ydbio.2008.03.028
Zhao, J., Kawai, K., Wang, H., Wu, D., Wang, M., Yue, Z., Zhang, J., Liu, Y.-H., 2012. Loss of Msx2 function down-regulates the FoxE3 expression and results in anterior segment dysgenesis resembling Peters anomaly. Am. J. Pathol. 180, 2230–2239. doi:10.1016/j.ajpath.2012.02.017

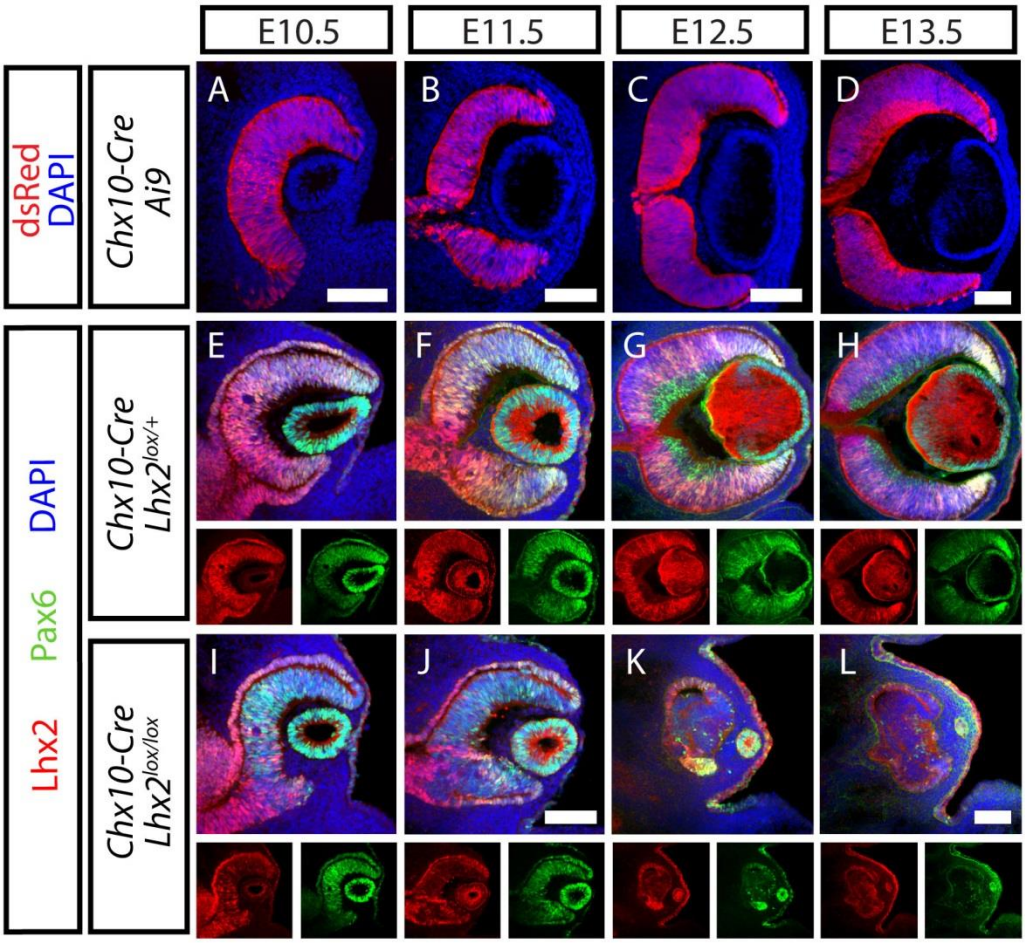

Supplemental Figure 1: Chx10-Cre is selectively active in the retina and eliminates Lhx2 expression in *Chx10-Cre;Lhx2$^{lox/lox}$* retinas. (A – D) Immunostaining for dsRed (red) to detect tdTomato expression in E10.5 – E13.5 *Chx10-Cre;Ai9* eye sections. (E – L) Immunostaining of *Chx10-Cre;Lhx2$^{lox/+}$* (E – H) and *Chx10-Cre;Lhx2$^{lox/lox}$* eye sections (I – L) for Lhx2 (red) and Pax6 (green). Nuclei are counter-stained with DAPI (blue). (Scale Bars: 100 µm)

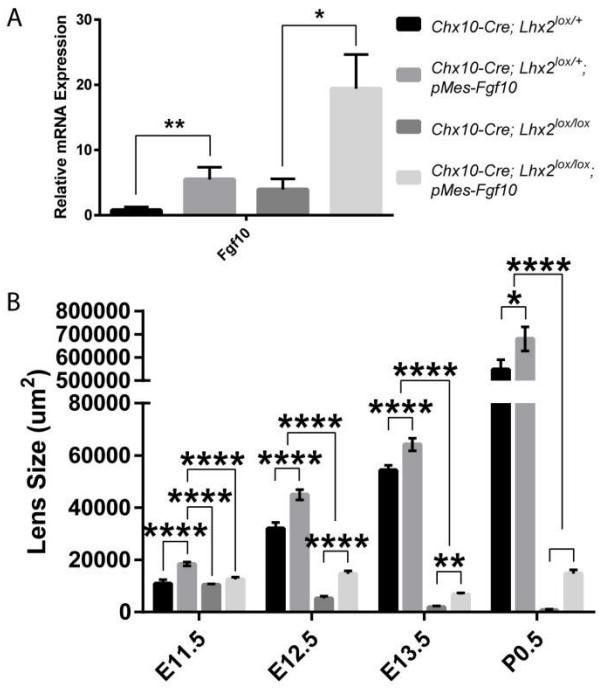

C

	No. of eyes with lens	No. of eyes without lens	Total
Chx10-Cre;Lhx2$^{lox/lox}$	5	6	11
Chx10-Cre;Lhx2$^{lox/lox}$; pMes-Fgf10	15	0	15
Total	20	6	26

Fisher's Exact Test: P = 0.002

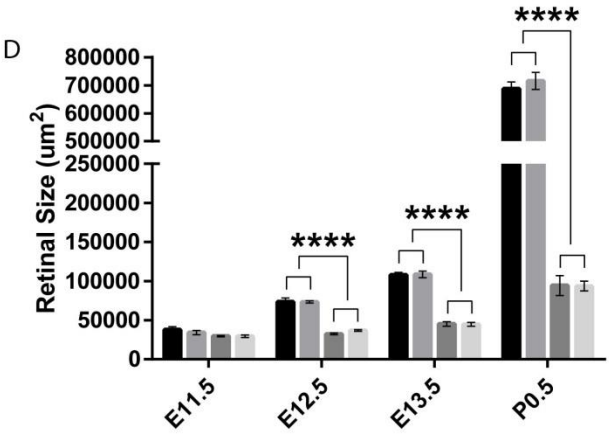

Supplemental Figure 2: Overexpression of *Fgf10* led to significant increase in lens, but not retinal, size. (A) Real-time quantitative PCR analysis shows induction of *Fgf10* mRNA expressions in *pMes-Fgf10* retinas. Data represent mean normalized to *Gapdh* values ± SEM. (Unpaired two-tailed t-test; n = 3; *P<0.05; **P<0.01) (B) Graph indicating the average lens size of *Chx10-Cre;Lhx2$^{lox/+}$*, *Chx10-Cre;Lhx2$^{lox/+}$;pMes-Fgf10*, *Chx10-Cre;Lhx2$^{lox/lox}$* and *Chx10-Cre;Lhx2$^{lox/lox}$;pMes-Fgf10* animals at E11.5, E12.5, E13.5 and P0.5. (C) Contingency table depicting the number of eyes with or without detectable lenses at P0.5 for *Chx10-Cre;Lhx2$^{lox/lox}$* and *Chx10-Cre;Lhx2$^{lox/lox}$;pMes-Fgf10* animals. Eye sections immunostained for Prox1 and β-Crystallin were used in this analysis. (D) Graph indicating average retinal area of *Chx10-Cre;Lhx2$^{lox/+}$*, *Chx10-Cre;Lhx2$^{lox/+}$;pMes-Fgf10*, *Chx10-Cre;Lhx2$^{lox/lox}$* and *Chx10-Cre;Lhx2$^{lox/lox}$;pMes-Fgf10* animals at E11.5, E12.5, E13.5 and P0.5. (One-way ANOVA followed by *post hoc* Tukey's test; n ≥ 4 for E11.5; n ≥ 9 for E12.5; n ≥ 6 for E13.5; n ≥ 7 for P0.5; *P<0.05; **P<0.01; ****P<0.0001; Error bars indicate SEM)

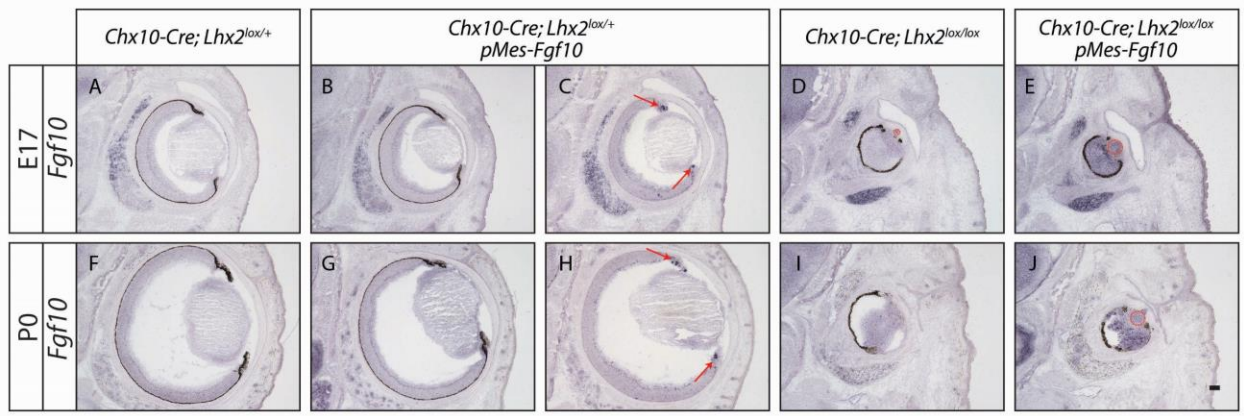

Supplemental Figure 3: Cre-mediated induction of *Fgf10* expression in *Chx10-Cre;Lhx2$^{lox/lox}$;pMes-Fgf10* retinas at later developmental stages. *In situ* hybridization analysis of *Fgf10* mRNA expression levels at E17 (A – E) and P0 (F – J). Sections from non-pigmented eyes were included in C and H to show the expression of Fgf10 in peripheral neuroretina in *Chx10-Cre;Lhx2$^{lox/+}$; pMes-Fgf10* eyes (red arrows). Dotted red circles mark the lenses (D, E and J). (Scale Bars: 100 µm)

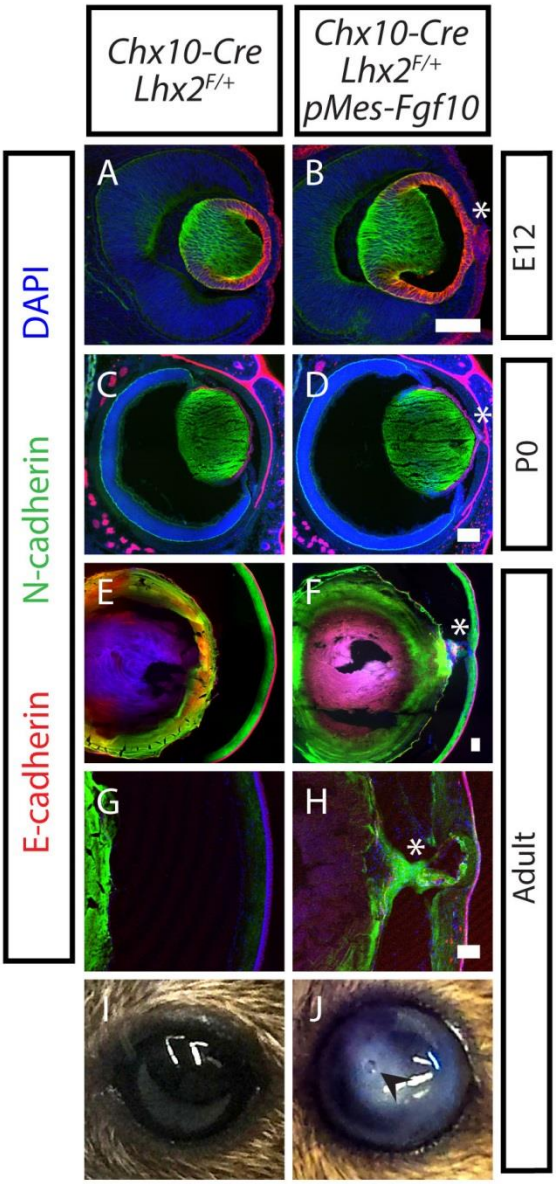

Supplemental Figure 4: *Fgf10* overexpression in control background led to tethering of lens to the cornea. (A – H) Eye sections of *Chx10-Cre;Lhx2*$^{lox/+}$ and *Chx10-Cre;Lhx2*$^{lox/+}$*;pMes-Fgf10* animals immunostained with E-cadherin (red) and N-cadherin (green). Nuclei are counter-stained with DAPI (blue). White asterisks indicate persistent lens stalks seen in *Chx10-Cre;Lhx2*$^{lox/+}$*; pMes-Fgf10* eyes (B, D, F and H). (I and J) External eye photos showing cornea opacification observed in some *Chx10-Cre;Lhx2*$^{lox/+}$*;pMes-Fgf10* animals (J). The anchor point of the lens stalk in the *Chx10-Cre;Lhx2*$^{lox/+}$*;pMes-Fgf10* animal could be detected in the image (J; black notched arrowhead).

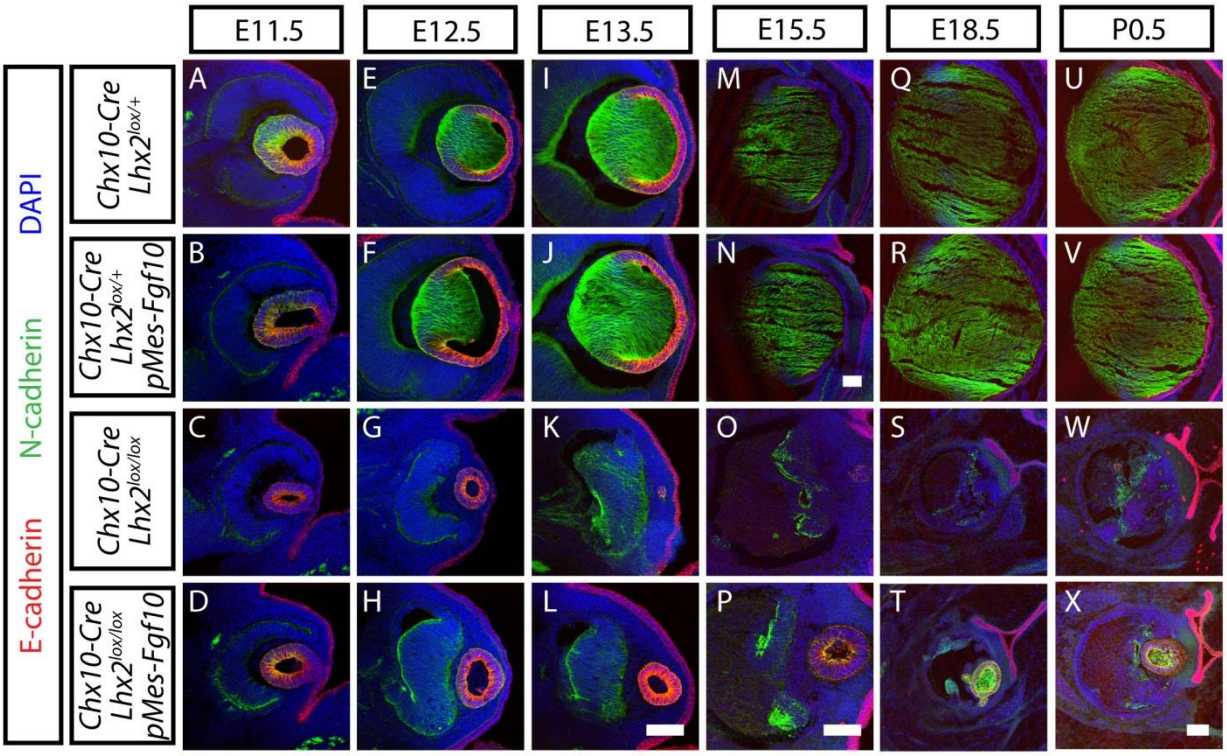

Supplemental Figure 5: *Chx10-Cre;Lhx2$^{lox/lox}$;pMes-Fgf10* rescue animals expressed lens epithelial cell marker E-cadherin and the lens fiber cell marker N-cadherin. Developmental time-course of immunohistochemistry for N-cadherin (green) and E-cadherin (red) expression in lenses at E11.5 (A – D), E12.5 (E – H), E13.5 (I – L), E15.5 (M – P), E18.5 (Q – T) and P0.5 (U – X) of *Chx10-Cre;Lhx2$^{lox/+}$* (A, E, I, M, Q, U), *Chx10-Cre;Lhx2$^{lox/+}$;pMes-Fgf10* (B, F, J, N, R, V), *Chx10-Cre;Lhx2$^{lox/lox}$* (C, G, K, O, S, W) and *Chx10-Cre;Lhx2$^{lox/lox}$;pMes-Fgf10* animals (D, H, L, P, T, X). Nuclei are counter-stained with DAPI (blue). (Scale Bars: 100 µm)

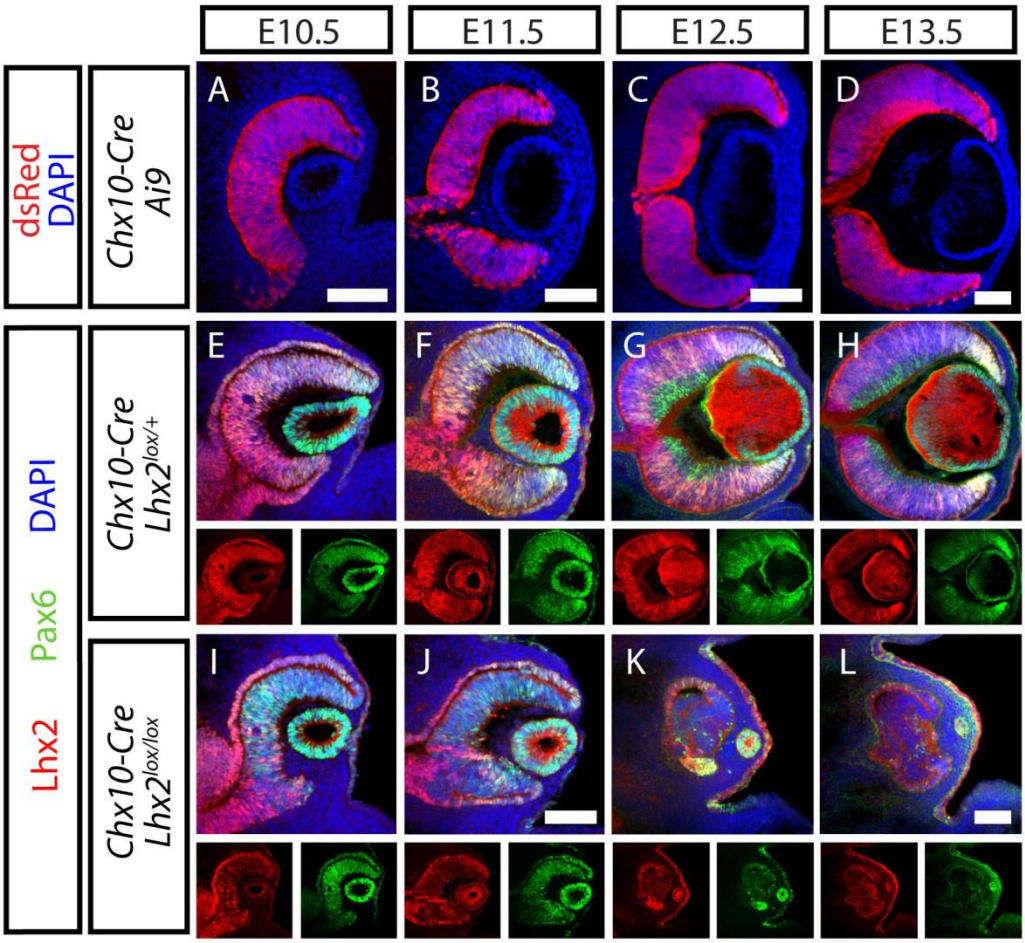

Supplemental Figure 1: Chx10-Cre is selectively active in the retina and eliminates Lhx2 expression in *Chx10-Cre;Lhx2$^{lox/lox}$* retinas. (A – D) Immunostaining for dsRed (red) to detect tdTomato expression in E10.5 – E13.5 *Chx10-Cre;Ai9* eye sections. (E – L) Immunostaining of *Chx10-Cre;Lhx2$^{lox/+}$* (E – H) and *Chx10-Cre;Lhx2$^{lox/lox}$* eye sections (I – L) for Lhx2 (red) and Pax6 (green). Nuclei are counter-stained with DAPI (blue). (Scale Bars: 100 µm)

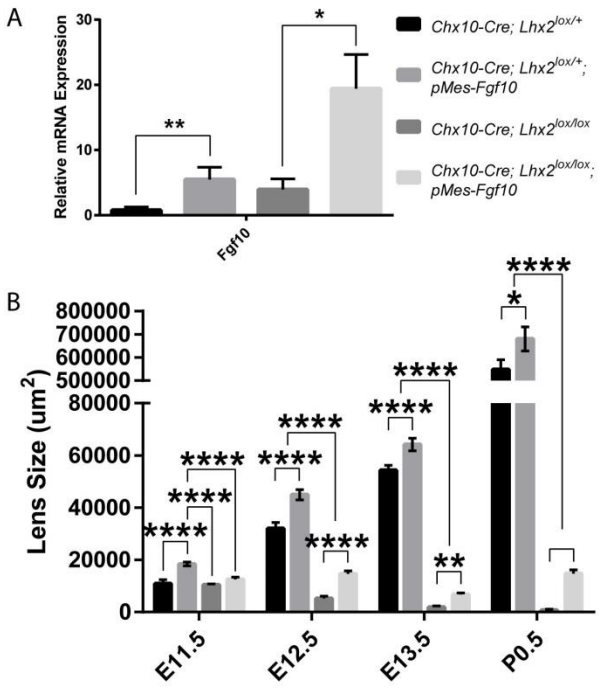

C

	No. of eyes with lens	No. of eyes without lens	Total
Chx10-Cre;Lhx2$^{lox/lox}$	5	6	11
Chx10-Cre;Lhx2$^{lox/lox}$; pMes-Fgf10	15	0	15
Total	20	6	26

Fisher's Exact Test: P = 0.002

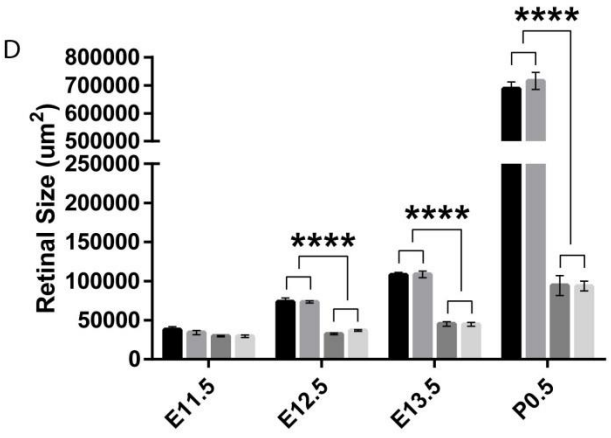

Supplemental Figure 2: Overexpression of *Fgf10* led to significant increase in lens, but not retinal, size. (A) Real-time quantitative PCR analysis shows induction of *Fgf10* mRNA expressions in *pMes-Fgf10* retinas. Data represent mean normalized to *Gapdh* values ± SEM. (Unpaired two-tailed t-test; n = 3; *P<0.05; **P<0.01) (B) Graph indicating the average lens size of *Chx10-Cre;Lhx2$^{lox/+}$*, *Chx10-Cre;Lhx2$^{lox/+}$;pMes-Fgf10*, *Chx10-Cre;Lhx2$^{lox/lox}$* and *Chx10-Cre;Lhx2$^{lox/lox}$;pMes-Fgf10* animals at E11.5, E12.5, E13.5 and P0.5. (C) Contingency table depicting the number of eyes with or without detectable lenses at P0.5 for *Chx10-Cre;Lhx2$^{lox/lox}$* and *Chx10-Cre;Lhx2$^{lox/lox}$;pMes-Fgf10* animals. Eye sections immunostained for Prox1 and β-Crystallin were used in this analysis. (D) Graph indicating average retinal area of *Chx10-Cre;Lhx2$^{lox/+}$*, *Chx10-Cre;Lhx2$^{lox/+}$;pMes-Fgf10*, *Chx10-Cre;Lhx2$^{lox/lox}$* and *Chx10-Cre;Lhx2$^{lox/lox}$;pMes-Fgf10* animals at E11.5, E12.5, E13.5 and P0.5. (One-way ANOVA followed by *post hoc* Tukey's test; n ≥ 4 for E11.5; n ≥ 9 for E12.5; n ≥ 6 for E13.5; n ≥ 7 for P0.5; *P<0.05; **P<0.01; ****P<0.0001; Error bars indicate SEM)

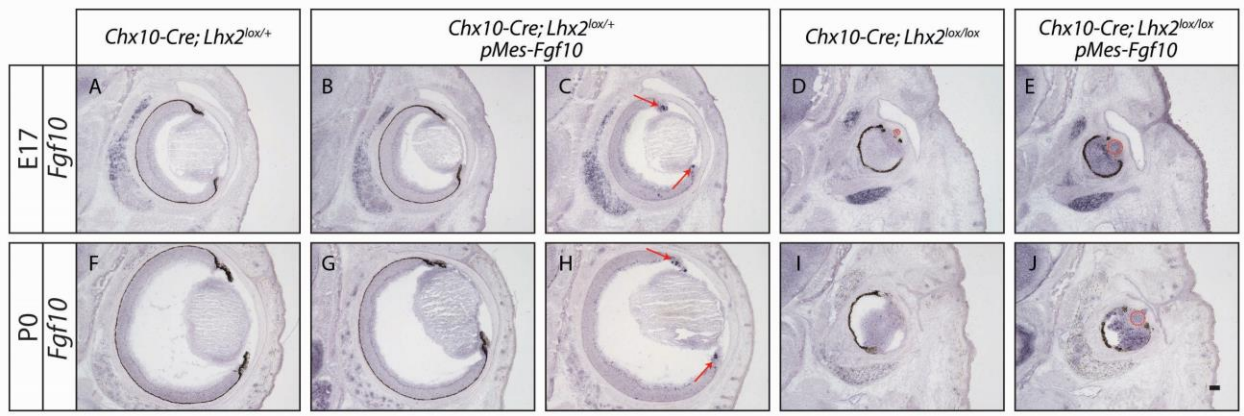

Supplemental Figure 3: Cre-mediated induction of *Fgf10* expression in *Chx10-Cre;Lhx2$^{lox/lox}$;pMes-Fgf10* retinas at later developmental stages. *In situ* hybridization analysis of *Fgf10* mRNA expression levels at E17 (A – E) and P0 (F – J). Sections from non-pigmented eyes were included in C and H to show the expression of Fgf10 in peripheral neuroretina in *Chx10-Cre;Lhx2$^{lox/+}$; pMes-Fgf10* eyes (red arrows). Dotted red circles mark the lenses (D, E and J). (Scale Bars: 100 µm)

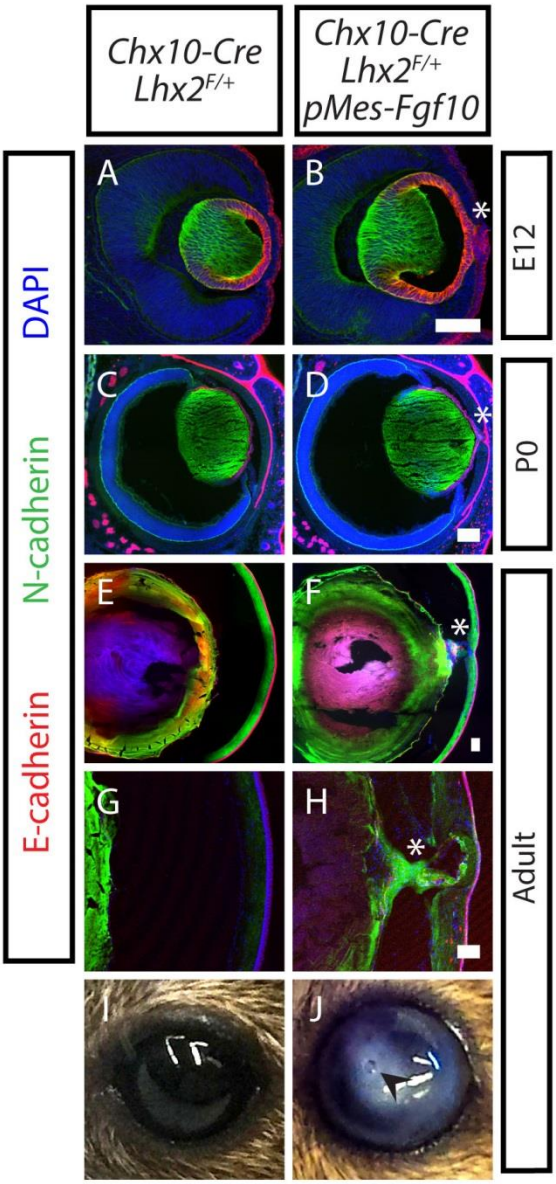

Supplemental Figure 4: *Fgf10* overexpression in control background led to tethering of lens to the cornea. (A – H) Eye sections of *Chx10-Cre;Lhx2*$^{lox/+}$ and *Chx10-Cre;Lhx2*$^{lox/+}$*;pMes-Fgf10* animals immunostained with E-cadherin (red) and N-cadherin (green). Nuclei are counter-stained with DAPI (blue). White asterisks indicate persistent lens stalks seen in *Chx10-Cre;Lhx2*$^{lox/+}$*; pMes-Fgf10* eyes (B, D, F and H). (I and J) External eye photos showing cornea opacification observed in some *Chx10-Cre;Lhx2*$^{lox/+}$*;pMes-Fgf10* animals (J). The anchor point of the lens stalk in the *Chx10-Cre;Lhx2*$^{lox/+}$*;pMes-Fgf10* animal could be detected in the image (J; black notched arrowhead).

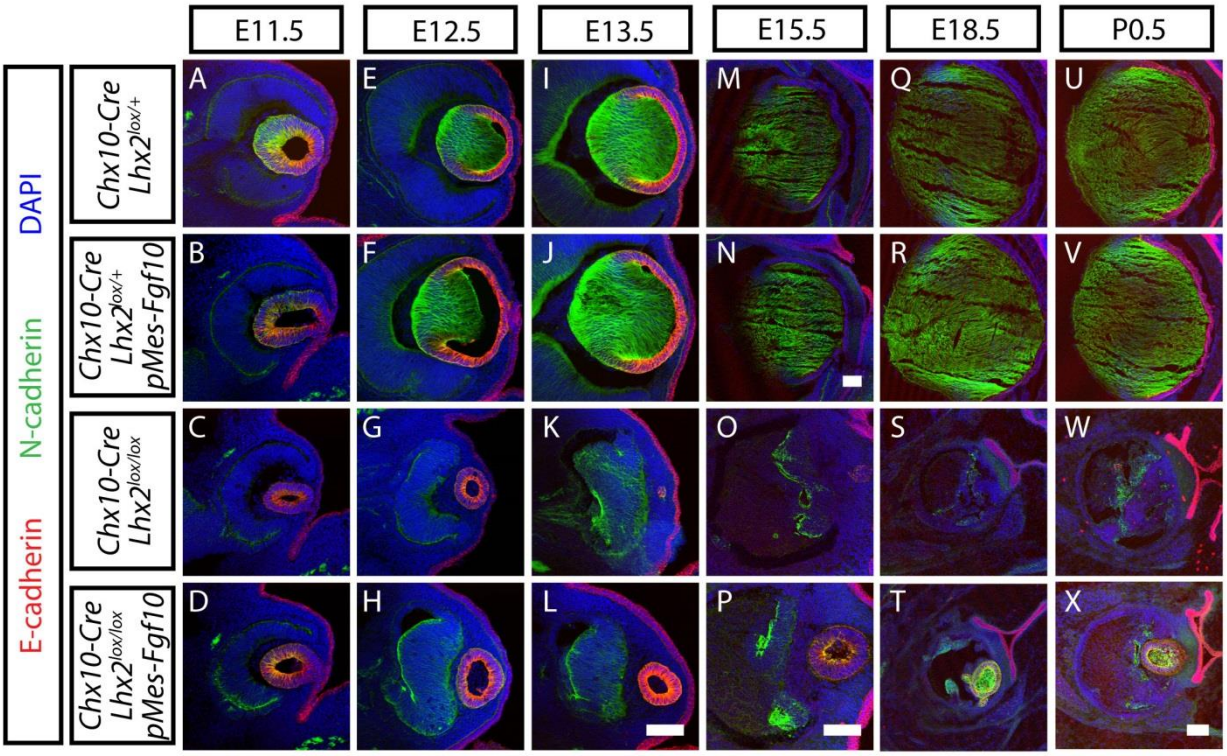

Supplemental Figure 5: *Chx10-Cre;Lhx2$^{lox/lox}$;pMes-Fgf10* rescue animals expressed lens epithelial cell marker E-cadherin and the lens fiber cell marker N-cadherin. Developmental time-course of immunohistochemistry for N-cadherin (green) and E-cadherin (red) expression in lenses at E11.5 (A – D), E12.5 (E – H), E13.5 (I – L), E15.5 (M – P), E18.5 (Q – T) and P0.5 (U – X) of *Chx10-Cre;Lhx2$^{lox/+}$* (A, E, I, M, Q, U), *Chx10-Cre;Lhx2$^{lox/+}$;pMes-Fgf10* (B, F, J, N, R, V), *Chx10-Cre;Lhx2$^{lox/lox}$* (C, G, K, O, S, W) and *Chx10-Cre;Lhx2$^{lox/lox}$;pMes-Fgf10* animals (D, H, L, P, T, X). Nuclei are counter-stained with DAPI (blue). (Scale Bars: 100 µm)